Med Chem Res
DOI 10.1007/s00044-017-2053-0

MEDICINAL CHEMISTRY RESEARCH

ORIGINAL RESEARCH

Antiplatelet activity, molecular docking and QSAR study of novel *N′*-arylmethylidene-3-methyl-1-phenyl-6-*p*-chlorophenyl-1*H*-pyrazolo[3,4-*b*] pyridine-4-carbohydrazides

Ayesha Ramzan[1] · Sara Siddiqui[1] · Ahmad Irfan[2,3] · Abdullah G. Al-Sehemi[2,3] · Aftab Ahmad[4] · Francis Verpoort[5] · Adeel H. Chughtai[5,6] · Misbahul A. Khan[1,7] · Munawar A. Munawar[1] · Muhammad Asim Raza Basra[1]

Received: 2 May 2017 / Accepted: 28 August 2017

Abstract A series of novel *N′*-arylmethylidene-3-methyl-1-phenyl-6-*p*-chlorophenyl-1*H*-pyrazolo[3,4-*b*]pyridine-4-carbohydrazide (**2a–2t**) has been synthesized from hydrazide (**1**). The structures of newly synthesized compounds were confirmed by FT-IR, EI-MS, ^{1}H NMR and ^{13}C NMR techniques. The title compounds were evaluated for antioxidant and antiplatelet aggregation effect induced by arachidonic acid (AA) and collagen. All the compounds have exhibited high antioxidant potential and antiplatelet activity but (**2c**, **2e**, **2f**, **2g**, **2i**, **2m**, **2o** and **2q**) have revealed superlative antiplatelet activity. The molecular docking against cyclooxygenase-1 and 2 (COX-1 and COX-2) and quantitative structure-activity relationship (QSAR) were performed in describing their antiplatelet potential against AA and collagen along with antioxidant potential determined by ABTS, DPPH and iron chelating methods. The molecular docking study exhibited that compounds (**2c**, **2e**, **2f**, **2g**, **2i**, **2l**, **2m**, **2o** and **2q**) were found to be active against COX-1 while **2o** compound also showed activity against COX-2. Compounds **2g** and **2l** were found to have higher energy stabilization values in comparison to Aspirin. Computational evaluations both molecular docking and QSAR are in good agreement with antiplatelet and antioxidant activities of the compounds (**2a–2t**). All the compounds especially **2g**, **2l**, **2m** might be promising antiplatelet agents and might be helpful in the synthesis of new drugs for the treatment of cardiovascular and anti-inflammatory diseases.

Electronic supplementary material The online version of this article (https://doi.org/10.1007/s00044-017-2053-0) contains supplementary material, which is available to authorized users.

✉ Misbahul A. Khan
misbahakhan@gmail.com

✉ Munawar A. Munawar
mamunawar.chem@pu.edu.pk
munawaralimunawar@yahoo.com

✉ Muhammad Asim Raza Basra
asimbasra@gmail.com
asimbasra.chem@pu.edu.pk

[1] Institute of Chemistry, University of the Punjab, Lahore 54590, Pakistan

[2] Department of Chemistry, Faculty of Science, King Khalid University, P.O. Box 9004, Abha 61413, Saudi Arabia

[3] Research Center for Advanced Materials Science (RCAMS), King Khalid University, P.O. Box 9004, Abha 61413, Saudi Arabia

[4] Center of Excellence in Molecular Biology, University of the Punjab, Lahore, Pakistan

[5] Laboratory of Organometallics, Catalysis, and Ordered Materials, State Key Laboratory of Advanced Technology for Materials Synthesis and Processing, Wuhan University of Technology, Wuhan 430070, China

[6] Institute of Chemical Sciences, Bahauddin Zakariya University, Multan 60800, Pakistan

[7] Department of Chemistry, The Islamia University of Bahawalpur, Bahawalpur, Pakistan

Published online: 20 September 2017

Graphical Abstract

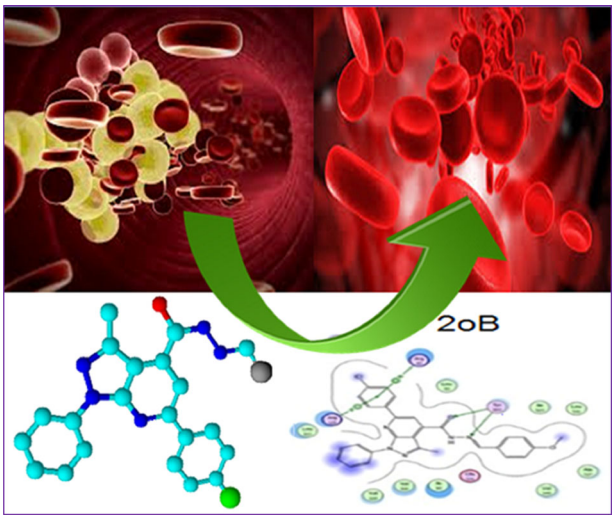

Keywords Acyl Hydrazone · Density Functional Theory · Electrostatic Potentiał · Physiochemical Properties

Introduction

Thrombotic disorders, e.g., myocardial infarction, peripheral vascular disease, stroke and angina are all caused by a common primary factor, i.e., platelet adhesion and aggregation, which played an important role in clot formation (Reddy et al. 2011). Keeping in view, research intention has been diverted toward selective inhibition of AA and collagen by binding with interactive residue of COX pocket. Many structure transformation of *N*′-acylhydrazones have been done by a number of researchers to enhance the antiplatelet activity (Haj Mohammad Ebrahim Tehrani et al. 2013).

Hydrazones have immense significance by virtue of their disparate biological applications, such as antimicrobial, antidiabetic, anticonvulsant, analgesic, antidepressant, anti-inflammatory, antiplatelet, antimalarial, antimycobacterial, vasodilator, anticancer, anti-HIV, and antiviral activities (Abdel-Wahab et al. 2011; Abu-Surrah et al. 2010; Ajani et al. 2010; Bezerra-Netto et al. 2006; de Aguiar Cordeiro et al. 2016; Magda et al. 2011; Patole et al. 2003; Salgın-Gökşen et al. 2007; Seleem et al. 2011; Sriram et al. 2005). Some of hydrazones are reported as antichagasic agents such as *N*′-(4-nitrobenzylidene)-3-methyl-1-phenyl-6-*p*-hydroxyphenyl-1*H*-pyrazolo[3,4-*b*]pyridine-4-carbohydrazide has exhibited highest antichagasic activity (Dias et al. 2007) while others are known for enzyme inhibition activities, (Abdelazem et al. 2015) still some are important in displaying antiplatelet activity as *N*′-(benzylidene)-3-methyl-1,6-diphenyl-1*H*-pyrazolo[3,4-*b*]pyridine-4-carbohydrazide has displayed excellent antiplatelet activity (Geraldo et al. 2010).

Hydrazones belong to imperative and influential group of compounds for useful novel and contemporary drug development. Now a days researchers have prepared a number of hydrazones and checked their various biological activities (Singh and Raghav 2011). Computational approaches have been broadly used to figure out and anticipate the potential capabilities of enzyme, ligand and their interactions. The leading computational methods include pharmacophore, three-dimensional QSAR and SAR analysis, molecular dynamics, homology modeling studies, simple rule-based modeling, and molecular docking (Hutter 2009).

In the present study, we have made an attempt toward the search of new potent COX inhibitors as antiplatelet drug with improved efficacy, and performed a SAR study. We synthesized a series of novel *N*′-benzylidene-3-methyl-1-phenyl-6-*p*-chlorophenyl-1*H*-pyrazolo[3,4*b*]pyridine-4-carbohydrazides (**2a–2t**) and then evaluated their potential antioxidant and antiplatelet activities. All the compounds have exhibited high antioxidant potential and antiplatelet activity. Docking studies were also performed against COX-1 and COX-2, and QSAR analysis was used to find out the binding interaction of synthesized compounds with the receptor in comparison to the standard drug Aspirin, in describing the antiplatelet potential of synthesized compounds. The aim of this study was to design, synthesize and investigate QSAR correlation along with molecular docking in order to develop new potent and selective platelet anti-aggregating drugs.

Materials and methods

Chemistry

All chemicals were purchased from Sigma-Aldrich and other well reputed suppliers. The chemicals were used mostly as such however when required purified by standard techniques, i.e., distillation and recrystallization. FT-IR spectra were recorded on Agilent Technologies 41630 and ^{1}H NMR, ^{13}C NMR recorded on ACD/NMR processor academic edition at 500 and 125 MHz in dimethyl sulfoxide (DMSO), respectively. The EIMS Data were taken on JEOl MS. 600H-1 while the completion of reaction was monitored by silica gel 60 F_{254} TLC plate.

6-(4-chlorophenyl)-3-methyl-1-phenyl-1*H*-pyrazolo[3,4-*b*] pyridine-4-carbohydrazide (**1**) was prepared by the already reported methods (Dias et al. 2007; Geraldo et al. 2010).

Synthesis of N′-arylmethylidene-3-methyl-1-phenyl-6-p-chlorophenyl-1H-pyrazolo[3,4-b]pyridine-4–carbohydrazides ***(2a–2t)***

Targeted compounds (**2a–2t**) were synthesized by the reaction of 6-(4-chlorophenyl)-3-methyl-1-phenyl-1*H*-pyrazolo[3,4-b]pyridine-4-carbohydrazide (**1**) (0.37 g, 1 mmol) with substituted aromatic aldehydes (1 mmol), and heating under reflux for an hour in glacial acetic acid (5 mL). The precipitates formed during the reaction were filtered, washed with cold ethanol, and finally dried in oven at 100 °C. Recrystallization from absolute ethanol gave the product as yellow colored solids. Yield 25–98%. This method provided novel, direct and flexible access to diverse *N′*-arylmethylidene-3-methyl-1-phenyl-6-p-chlorophenyl-1*H*-pyrazolo[3,4-b]pyridine-4–carbohydrazides **(2a–2t)**.

N′-(Benzylidene)-3-methyl-1phenyl-6-p-chlorophenyl-1*H*-pyrazolo[3,4-b]pyridine-4-carbohydrazide (**2a**) Compound **2a** was prepared by the reaction of **1** with benzaldehyde. The yellow product was recrystallized from ethanol. Yield: 86%; m.p 260–262 °C; IR ν_{max}(cm^{-1}):3173 (N-H); 3062 (CH-Ar); 2965 (CH-Aliph); 1662 (C=O); 1603; 1573; (C=C); 687 (C-Cl):. ^{1}H NMR (500 MHz, DMSO-d_6): $\delta = 12.44_{ap}$, 12.28_{sp} (2 s, 1H, NH) 8.42_{sp}, 8.37_{ap} (2s, 1H, N=CH), $8.35_{(sp+ap)}$ (d, $J = 8.6$ Hz, 2H, H-2″, H-6″), $8.32_{(sp+ap)}$ (d, $J = 7.8$ Hz, 2H, H-2′, H-6′), 8.17_{sp}, 8.04_{ap} (2 s, 1H, H-5), $7.8_{(sp+ap)}$ (d, $J = 7.2$ Hz, 2H, H-2‴, H-6‴), $7.67_{(sp+ap)}$ (d, $J = 8.6$ Hz, 2H, H-3″, H-5″), $7.62_{(sp+ap)}$ (t, $J = 8.0$ Hz, 2H, H-3′, H-5′), 7.53–$7.36_{(sp+ap)}$ (m,3H, H-3‴, H-5‴, H-4′), 7.32–$7.25_{(sp+ap)}$ (m, 1H, H-4‴), 2.62 (s, 3H, CH_3). Rotamers percentage $sp_{(74\%)}$: $ap_{(26\%)}$. ^{13}C NMR (125 MHz, DMSO-d_6): $\delta = 168.1_{ap}$, 162.0_{sp} (C=O), 155.4 (C-6), 151.4 (C-7a), 149.5 (N=CH), 142.7 (C-3), 142.3 (C-4), 139.4_{sp}, 139.3_{ap}, (C-1′), 137.1 (C-1″), 135.6 (C-1‴), 134.4 (C-4″), 131.0 (C-4‴), 129.8 (C-3‴, 5″), 129.7 (C-3′, C-5′), 129.6 (C-2‴, C-6‴), 129.4 (C-2″, 6″), 127.8 (C-3‴, C-5‴), 127.2 (C-4′), 126.4 (C-5), 121.2_{sp}, 120.9_{ap}(C-2′, C-6′), 113 (C-3a), 15.0_{sp}, 13.7_{ap} (CH_3). MS (EI^+): *m/z* 465 (M+, 100%), 467 (M + 2, 40), 362 (46), 346 (60), 318 (52), 278 (9), 242 (25), 140 (7), 77 (13).

N′-(2-Nitrobenzylidene)-3-methyl-1phenyl-6-p-chlorophenyl-1*H*-pyrazolo[3,4-b]pyridine-4-carbohydrazide (**2b**) Compound **2b** was prepared by the reaction of **1** with 2-nitrobenzaldehyde. The yellow product was recrystallized from ethanol. Yield: 75%. m.p 272–274 °C; IR ν_{max} (cm^{-1}): 3181 (N-H); 3010 (CH-Ar); 2853 (CH-Aliph); 1655 (C=O); 1566, 1350 (NO_2) 1506 (C=C); 687 (C-Cl).^{1}H NMR (500 MHz, DMSO-d_6): $\delta = 12.79_{ap}$, 12.62_{sp} (2s, 1H, NH), 8.84_{sp}, 8.52_{ap} (2 s, 1H, N=CH), $8.36_{(sp+ap)}$ (d, $J =$ 8.6 Hz, 2H, H-2″, H-6″), $8.32_{(sp+ap)}$ (d, $J = 7.8$ Hz, 2H, H-2′, H-6′), 8.22_{sp}, 8.4_{ap} (2d, $J = 7.7$ Hz, 1H, H-5‴), 8.19_{sp}, 8.02_{ap} (2 s, 1H, H-5), $7.88_{(sp+ap)}$ (t, $J = 7.5$ Hz,1H, H-3‴), $7.68_{(sp+ap)}$ (d, $J = 8.6$ Hz 2H, H-3″, H-5″), $7.63_{(sp+ap)}$ (d, $J = 7.4$ Hz, 2H, H-3′, H-5′), 7.61_{ap}, 7.53_{sp} (m, 1H, H-4‴), $7.41_{(sp+ap)}$ (m, 1H, H-4′) $2.63_{(sp+ap)}$ (s, 3H, CH_3). Rotamers percentage $sp_{(73\%)}$: $ap_{(27\%)}$. ^{13}C NMR (125 MHz, DMSO-d_6): $\delta = 168.7_{ap}$, 162.3_{sp} (C=O), 155.4 (C-6),151.4 (C-7a), 148.8(C-2‴), 145.1 (N=CH), 142.7 (C-3), 139.3 (C-4), (138.8 C-1′), 137.0 (C-1″), 135.6 (C-5‴), 134.4 (C-4″), 131.6 (C-4‴), 129.8 (C-3″, C-5″), 129.7 (C-3′, C-5′), 129.6 (C-6‴), 129.5 (C-2″, C-6″), 128.9 (C-1‴), 128.7 (C-4′), 126.4 (C-5), 125.3_{ap}, 125.0_{sp}(C-3‴), 121.2_{sp}, 120.9_{ap}(C-2′, C-6′), 113.9 (C-3a), 15.0_{sp},13.6_{ap} (CH_3). MS (EI^+): *m/z* 510 (M+, 100%), 512 (M + 2, 40), 463 (47), 362 (31), 346 (90), 318 (95), 277 (15), 242 (34).

N′-(3-Nitrobenzylidene)-3-methyl-1phenyl-6-p-chlorophenyl-1*H*-pyrazolo[3,4-b]pyridine-4-carbohydrazide (**2c**) Compound **2c** was prepared by the reaction of **1** with 3-nitrobenzaldehyde. The yellow product was recrystallized from ethanol. Yield: 77%. m.p 270–272 °C; IR ν_{max} (cm^{-1}): 3188 (N-H); 3054 (CH-Ar); 2935 (CH-Aliph); 1.670 (C=O); 1603 (C=C); 1536, 1357 (NO_2); 687 (C-Cl). ^{1}H NMR (500 MHz, DMSO-d_6): $\delta = 12.69_{ap}$, 12.55_{sp} (2 s, 1H, NH), 8.63_{ap}, 8.54_{sp} (2 s, 1H, N=CH), 8.36–$8.35_{(sp+ap)}$ (m, 2H, H-2″, H-6″), $8.32_{(sp+ap)}$ (d, $J = 7.7$ Hz, 2H, H-2′, H-6′), 8.25_{sp}, 8.07_{ap} (d, $J = 7.8$ Hz 1H, H-6‴), 8.18_{sp}, 8.07_{ap} (2 s, 1H, H-5), 7.82_{sp}, 7.74_{ap} (t, $J = 8.9$ Hz, 1H, H-5‴), $7.67_{(sp+ap)}$ (d, $J = 8.6$ Hz 2H, H-3″, H-5″) $7.62_{(sp+ap)}$ (d, $J = 7$ Hz, 2H, H-3′, H-5′), $7.61_{(sp+ap)}$ (s, 1H, H-2‴), $7.57_{(sp+ap)}$ (t, $J = 7.8$ Hz, 1H, H-4‴), $7.38_{(sp+ap)}$ (m,1H, H-4′), $2.63_{(sp+ap)}$ (s, 3H, CH_3). Rotamers percentage $sp_{(77\%)}$: $ap_{(23\%)}$. ^{13}C NMR (125 MHz, DMSO-d_6): $\delta =$ 168.5_{ap}, 165.8_{sp} (C=O), 155.4 (C-6), 151.4 (C-7a), 148.8 (C-3‴), 147.2 (N=CH), 142.7 (C-3), 139.3 (C-4), 138.9 (C-1′), 137.0 (C-1″), 136.3 (C-1‴), 135.6 (C-6‴), 134.0 (C-4′′), 131.1 (C-5‴), 129.8 (C-3″, C-5″), 129.7 (C-3′, C-5′), 129.6(C-4‴), 121.8 (C-5), 121.2_{sp}, 121.0_{ap}(C-2′, 6′), 113.8, 112.3 (C-3a), 14.9_{sp}, 13.7_{ap} (CH_3). MS (EI^+): *m/z* 510 (M +, 100%), 512 (M + 2, 39), 480 (21), 362 (35), 346 (80), 318 (54), 277 (11), 242 (23).

N′-(4-Nitrobenzylidene)-3-methyl-1phenyl-6-p-chlorophenyl-1*H*-pyrazolo[3,4-b]pyridine-4-carbohydrazide (**2d**) Compound **2d** was prepared by the reaction of **1** with 4-nitrobenzaldehyde. The yellow product was recrystallized from ethanol. Yield: 85%. m.p300 °C; Lit. (Dias et al. 2007) [296–298 °C]; IR ν_{max} (cm^{-1}): 3213 (N–H); 3043 (CH-Ar); 2921 (CH-Aliph); 1.661 (C=O); 1594 (C=C); 1533, 1348 (NO_2); 687 (C–Cl). ^{1}H NMR (500 MHz, DMSO-d_6): $\delta = 12.73_{sp}$, 12.57_{ap} (2 s, 1H, NH), 8.52_{ap}, 8.36_{sp} (2 s, 1H, N=CH), $8.34_{(sp+ap)}$ (d, $J = 8.7$ Hz, 2H, H-2″, H-6″), $8.31_{(sp+ap)}$ (d, $J = 7.6$ Hz, 2H, H-2′, H-6′), 8.29_{sp}, 8.19_{ap} (2 s, 1H, H-5), $8.09_{(sp+ap)}$ (d, $J = 7.1$ Hz, 2H, H-2‴, H-6‴,

$7.67_{(sp+ap)}$ (d, $J = 8.6$ Hz, 2H, H-3″, H-5″), $7.62_{(sp+ap)}$ (t, $J = 8.0$ Hz, 2H, H-3′, H-5′), $7.38_{(sp+ap)}$ (t, $J = 7.4$ Hz, 1H, H-4′), $2.62_{(sp+ap)}$ (s, 3H, CH_3). Rotamers percentage $sp_{(77\%)}$: $ap_{(23\%)}$. ^{13}C NMR (125 MHz, DMSO-d_6): $\delta =$ 168.4_{ap}, 162.4_{sp} (C=O), 155.4 (C-6), 151.4(C-7a), 148.6 (C-4‴), 147.1 (N=CH), 142.7 (C-3), 140.6 (C-4), 139.3 (C-1‴), 138.8 (C-1′), 137.0 (C-1″), 135.6 (C-4″), 129.8 (C-3″, C-5″),129.7 (C-3′, C-5′), 129.6 (C-2″, C-6″), 128.8(C-4′), 128.1(C-2‴, C-6‴),126.4(C-3‴, C-5‴), 124.6 (C-5), 121.2_{sp},120.9_{ap}(C-2′, C-6′), 113.9 (C-3a), 14.9_{sp}, 13.6_{ap} (CH_3). MS (EI^+): *m/z* 510 (M+, 100%), 512 (M + 2, 41), 480 (10), 362 (13.4), 346 (87.8), 318 (55), 277 (9.5), 242 (22).

N′-(2-Bromobenzylidene)-6-(4-chlorophenyl)-3-methyl-1-phenyl-1*H*-pyrazolo[3,4-b]pyridine-4-carbohydrazide (**2e**) Compound **2e** was prepared by the reaction of **1** with 2-bromobenzaldehyde. The yellow product was recrystallized from ethanol. Yield: 86%. m.p 210–212 °C; IR ν_{max} (cm^{-1}): 3182 (N–H); 3066 (CH-Ar); 2925 (CH-Aliph); 1676 (C=O); 1597 (C=C); 690 (C–Cl). ^{1}H NMR (500 MHz, DMSO-d_6): $\delta = 11.63_{ap}$, 11.46_{sp} (2 s, 1H, NH), 10.70_{ap}, 10.19_{sp} (2 s, 1H, N=CH), 8.50_{ap}, 8.34_{sp} (2 s, 1H, H-5), $8.31_{(sp+ap)}$ (d, $J = 7.7$ Hz, 2H, H-2″, H-6″), $8.28_{(sp+ap)}$ (d, $J = 8.6$ Hz, 2H, H-2′, H-6′), 7.95–$7.90_{(sp+ap)}$ (m, 1H, H‴), $7.67_{(sp+ap)}$ (m,4H, H-3″, H-5″, H-3′, H-5′), $7.61_{(sp+ap)}$ (t, $J = 7.9$ Hz, 1H, H-4‴), 7.42-$7.45_{(sp+ap)}$ (m, 1H, H-4′), 7.39–$7.31_{(sp+ap)}$ (m, 2H, H-3‴, H-5‴), $2.63_{(sp+ap)}$ (s, 3H, CH_3). Rotamers percentage $sp_{(65\%)}$: $ap_{(35\%)}$. ^{13}C NMR (125 MHz, DMSO-d_6): $\delta = 168.9$, 166.2, 164.9_{sp}, 161.2_{ap} (C=O), 155.3 (C-6), 151.4 (C-7a), 144.3 (N=CH), 142.9 (C-3), 141.4 (C-4), 139.3 (C-1′), 138.9 (C-1″), 137.1_{ap}, 135.5_{sp}(C-1‴),133.6_{ap},133.5_{sp} (C-4″), 132.0 (C-3‴), 131.8 (C-4‴), 129.7 (C-3″, C-5″), 129.7 (C-3′, C-5′), 129.6 (C-2″, C-6″), 128.5 (C-5‴), 127.6_{ap}, 127.4_{sp}(C-6‴), 126.3 (C-4′), 123.8 (C-5), 123.6 (C-2‴), 121.1 (C-2′, C-6′), 113.4(C-3a), 14.9 (CH_3). MS (EI^+): *m/z* 543 (M+, 4%), 545 (M + 2, 5), 547 (M + 4, 2), 419 (73), 362 (12), 346 (100), 318 (80), 277 (10), 242 (22).

N′-(3-Bromobenzylidene)-6-(4-chlorophenyl)-3-methyl-1-phenyl-1*H*-pyrazolo[3,4-b]pyridine-4-carbohydrazide (**2f**) Compound **2f** was prepared by the reaction of **1** with 3-bromobenzaldehyde. The yellow product was recrystallized from ethanol. Yield: 97%. m.p 245–247 °C; IR ν_{max} (cm^{-1}): 3173 (N–H); 3047 (CH-Ar); 1656 (C=O); 1594; 1573; 1536 (C=C); 691 (C–Cl). ^{1}H NMR (500 MHz, DMSO-d_6): $\delta = 12.56_{ap}$, 12.4_{sp} (2 s, 1H, NH), 8.38_{sp} (s, 1H, N=CH), $8.35_{(sp+ap)}$ (d, $J = 3$H, N=CH_{ap}, H-2″, H-6 ″), $8.32_{(sp+ap)}$ (d, $J = 7.9$ Hz, 2H, H-2′, H-6′), 8.17_{sp}, 8.14_{ap} (2 s, 1H, H-5), 8.05_{ap}, 8.01_{sp} (2 s, 1H, H-2‴), $7.81_{(sp+ap)}$ (d, $J = 7.8$ Hz, 1H, H-6‴), $7.68_{(sp+ap)}$ (t, $J = 8.4$ Hz, H, H-3″, H-5″), $7.63_{(sp+ap)}$ (t, $J = 8.3$ Hz, 2H, H-3′, H-5′), $7.6_{(sp+ap)}$ (m, 1H, H-5‴), 7.51–7.35(m, 2H, H-4′, H-4‴), 2.62 (s, 3H, CH_3). Rotamers percentage $sp_{(82\%)}$: $ap_{(18\%)}$. ^{13}C NMR (125 MHz, DMSO-d_6): $\delta = 168.0_{ap}$, 162.2_{sp} (C=O), 155.4 (C-6), 151.4 (C-7a), 147.8 (N=CH), 142.7 (C-3), 139.3 (C-4), 139.1 (C-1′), 137.0 (C-1″), 136.9 (C-1″′), 135.6 (C-4″), 133.5_{sp}, 131.6_{ap} (C-4‴), 129.9 (C-3″, C-5″′), 129.8 (C-3′, C-5′), 129.7 (C-2‴, C-6‴), 129.6 (C-2″, C-6″′), 126.9 (C-4′), 126.4 (C-5), 122.7 (C-3‴), 121.2 (C-2′, C-6′), 121.0 (C-5), 113.8 (C-3a), 14.9_{sp}, 13.6_{ap} (CH_3). MS (EI^+): *m/z* 543 (M+, 76%), 545 (M + 2, 100), 547 (M + 4, 27), 362 (43), 346 (92), 318 (61), 277 (9), 242 (19).

N′-(4-Bromobenzylidene)-6-(4-chlorophenyl)-3-methyl-1-phenyl-1*H*-pyrazolo[3,4-b]pyridine-4-carbohydrazide (**2g**) Compound **2g** was prepared by the reaction of **1** with 4-brombenzaldehyde. The yellow product was recrystallized from ethanol. Yield: 84%. m.p 285–287 °C; IR ν_{max} (cm^{-1}): 3182 (N–H); 3053 (CH-Ar); 2960 (CH-Aliph); 1656 (C=O); 1560 (C=C); 681 (C–Cl). ^{1}H NMR (500 MHz, DMSO-d_6): $\delta = 12.50_{ap}$, 12.35_{sp} (2 s, 1H, NH), 8.39_{sp}, 8.36_{ap} (2 s, 1H, N=CH), $8.34_{(sp+ap)}$ (d, $J = 8.6$ Hz, 2H, H-2″, H-6″), $8.32_{(sp+ap)}$ (d, $J = 8.3$ Hz, 2H, H-2′, H-6′), 8.17_{sp}, 8.03_{ap} (2 s, 1H, H-5), 7.83_{ap}, 7.76_{sp} (d, $J = 8.5$ Hz, 2H, H-2‴, H-6‴) $7.71_{(sp+ap)}$ (d, $J = 8.5$ Hz, 2H, H-3‴, H-5‴) $7.67_{(sp+ap)}$ (d, $J = 8.6$ Hz, 2H, H-3″, H-5″), 7.50–$7.23_{(sp+ap)}$ (m,3H, H-3′, H-5′, H-4′), 2.61 (s, 3H, CH_3). Rotamers percentage $sp_{(72\%)}$: $ap_{(28\%)}$. ^{13}C NMR (125 MHz, DMSO-d_6): $\delta = 168.0_{sp}$,162.1_{ap} (C=O), 155.4 (C-6), 151.4 (C-7a), 148.3 (N=CH), 142.7 (C-3), 139.3 (C-4), 139.1 (C-1′), 137.0 (C-1″), 135.6 (C-1‴), 133.7 (C-4″), 132.4 (C-4′), 129.8 (C-3″, C-5″), 129.7 (3′, 5′), 129.6 (C-2″′, C-6‴), 129.1 (C-2″, C-6″), 126.4 (C-3‴, 5‴), 124.3 (C-4″′), 121.2 (C-2′, C-6′), 120.9 (C-5), 113.8 (C-3a), 14.9_{sp}, 13.7_{ap} (CH_3). MS (EI^+): m/z 543 (M+, 70%), 545 (M + 2, 91), 547 (M + 4, 27), 362 (46), 346 (100), 318 (75), 277 (14), 242 (39).

N′-(2-Flourobenzylidene)-6-(4-chlorophenyl)-3-methyl-1-phenyl-1*H*-pyrazolo[3,4-b]pyridine-4-carbohydrazide (**2h**) Compound **2h** was prepared by the reaction of **1** with 2-flourobenzaldehyde. The yellow product was recrystallized from ethanol. Yield: 76%. m.p 265–267 °C; IR: ν_{max} ($cm^{-1)}$: 3295 (N–H); 3065 (CH-Ar); 2966 (CH-Aliph); 1662 (C=O); 1594; 1572; 1507 (C=C); 680 (C-Cl). ^{1}H NMR (500 MHz, DMSO-d_6): $\delta = 12.54_{ap}$, 12.4_{sp} (2 s, 1H, NH), 8.65_{sp}, 8.38_{ap} (2 s, 1H, N=CH), $8.36_{(sp+ap)}$ (d, $J =$ 8.4 Hz, 2H, H-2″, H-6″), $8.32_{(sp+ap)}$ (d, $J = 7.8$ Hz, 2H, H-2′, H-6′), 8.20_{sp} (s, 1H, H-5), 8.03–$8.04_{(sp+ap)}$ (m, 2H, H-5_{ap}, H-6‴), $7.68_{(sp+ap)}$ (d, $J = 8.4$ Hz, 2H, H-3″, H-5‴), 7.61 (t, $J = 7.9$ Hz, 2H, H-3′, H-5′), 7.59–$7.32_{(sp+ap)}$ (m, 3H, H-3‴, H-5‴, H-4′), 7.25–$7.00_{(sp+ap)}$ (m, 1H, H-4‴) 2.63_{ap} (s, 3H, CH_3). Rotamers percentage $sp_{(74\%)}$: $ap_{(26\%)}$. ^{13}C NMR (125 MHz, DMSO-d_6): $\delta = 165.1_{sp}$, 162.1_{ap}

(C=O), 155 (C-2‴), 151.7 (C-6), 151.4 (C-7a), 142.6 (C-3), 139.1 (C-4), 138.8 (C-1′), 129.8 (C-1″), 129.6 (C-4″), 127.6 (C-4‴), 126.9 (C-3″, C-5″), 126.5 (3′, 5′), 125.6 (C-6‴), 121.2 (C-2″, C-6″), 114.3 (C-5), 113.6 (C-2′, 6′), 112.4 (C-3a), 15.0_{sp},13.9_{ap} (CH_3). MS (EI^+): *m/z* 483 (M+, 100%), 485 (M + 2, 23), 463 (25), 362 (22), 346 (61), 318 (60), 277 (7), 242 (19).

N′-(3-Flourobenzylidene)-6-(4-chlorophenyl)-3-methyl-1-phenyl-1*H*-pyrazolo[3,4-b]pyridine-4-carbohydrazide (**2i**) Compound **2i** was prepared by the reaction of **1** with 3-flourobenzaldehyde. The yellow product was recrystallized from ethanol. Yield: 97%. m.p 267–270 °C; IR ν_{max} (cm^{-1}): 3178 (N–H); 3065 (CH-Ar); 2970 (CH-Aliph); 1663 (C=O); 1595; 1575; 1507 (C=C); 1351 (F); 689 (Cl). ^{1}H NMR (500 MHz, DMSO-d_6): $\delta = 12.57_{sp}$, 12.39_{ap} (2 s, 1H, NH), $8.42_{(sp+ap)}$ (s, 1H, N=CH), $8.35_{(sp+ap)}$ (d, J = 8.6 Hz, 2H, H-2″, H-6″), $8.32_{(sp+ap)}$ (d, $J = 7.6$ Hz, 2H, H-2′, H-6′), 8.17_{sp}, 8.04_{ap} (2 s, 1H, H-5), $7.67_{(sp+ap)}$ (d, J = 8.5 Hz, 2H, H-3″, H-5″), $7.63_{(sp+ap)}$ (dd, $J = 14.1$, 5.8 Hz, 2H, H-3′, H-5′), $7.56_{(sp+ap)}$ (dd, $J = 13.9$, 7.9 Hz, 2H, H-3‴, H-5‴), $7.38_{(sp+ap)}$ (t, $J = 7.3$ Hz, 1H, H-4′), 7.36–7.31 (m, 1H, H-4‴), 2.62 (s, 3H, CH_3). Rotamers percentage $sp_{(80\%)}$: $ap_{(20\%)}$. ^{13}C NMR (125 MHz, DMSO-d_6): $\delta = 163.8_{sp}$, 162.1_{ap} (C=O), 162.0 (C-3‴), 155.4 (C-6), 151.4 (C-7a), 147.9 (N=CH), 142.7 (C-3), 139.3 (C-4), 139.1 (C-1′), 137.0 (C-1″), 135.6 (C-1‴), 131.6 (C-4″), 129.8 (C-3″, C-5″), 129.7 (C-3′, C-5′), 129.6 (C-2″, C-6″), 126.4 (C-4′), 124.2 (C-6‴), 121.2 (C-2′, C-6′), 120.9 (C-5‴), 117.7 (C-4‴), 113.9 (C-2‴), 113.8 (C-5), 113.7 (C-3a), 14.9_{sp}, 13.6_{ap} (CH_3). MS (EI^+): *m/z* 483 (M+, 100%), 485 (M + 2, 45), 362 (25), 346 (89), 318 (70), 277 (10), 242 (27).

N′-(4-Flourobenzylidene)-6-(4-chlorophenyl)-3-methyl-1-phenyl-1*H*-pyrazolo[3,4-b]pyridine-4-carbohydrazide (**2j**) Compound **2j** was prepared by the reaction of **1** with 4-flourobenzaldehyde. The yellow product was recrystallized from ethanol. Yield: 97%. m.p 269–271 °C; Lit (Dias et al. 2007) [230 °C]. IR ν_{max} (cm^{-1}): 3185(N–H); 3062 (CH-Ar); 2900 (CH-Aliph); 1.655 (C=O); 1595 (C=C); 691 (C–Cl). ^{1}H NMR (500 MHz, DMSO-d_6): $\delta = 12.45_{sp}$, 12.29_{ap} (2 s, 1H, NH), 8.41_{ap}, 8.37_{sp} (2 s, 1H, N=CH), $8.36_{(sp+ap)}$ (d, $J = 4.4$ Hz, 2H, H-2″, H-6″), $8.33_{(sp+ap)}$ (d, $J = 12.6$, 8.5 Hz, 2H, H-2′, H-6′), 8.16_{ap}, 8.02_{sp} (2s, 1H, H-5), $7.87_{(sp+ap)}$ (d, $J = 8.67$, 5.7 Hz, 2H, H-2‴, H-6‴) $7.67_{(sp+ap)}$ (d, $J = 8.6$ Hz, 2H, H-3″, H-5″), $7.62_{(sp+ap)}$ (t, $J = 8.0$ Hz, 2H, H-3′, H-5′), $7.35_{(sp+ap)}$ (m, 2H, H-3‴, H-5‴), $7.12_{(sp+ap)}$ (t, $J = 8.8$ Hz, 1H, H-4′), $2.62_{(sp+ap)}$ (s, 3H, CH_3). Rotamers percentage $ap_{(77\%)}$: $sp_{(23\%)}$. ^{13}C NMR (125 MHz, DMSO-d_6): $\delta = 165.2$ (C-4‴), 163.0_{ap}, 162.1_{sp} (C=O), 155.4 (C-6), 151.4 (C-7a), 148.4 (N=CH), 144.8_{ap}, 142.7_{sp}(C-3), 140.4 (C-4), 139.3(C-1′), 139.2(C-1″), 137.0_{sp},135.6_{ap}(C-1‴), 131.3 (C-4″), 130.1 (C-2‴, C-6‴), 129.8(C-3″, C-5″, 129.7) (C-3′, C-5′), 129.6 (C-2″, C-6″), 126.4 (C-4′), 121.2_{sp}, 120.9_{ap} (C-5), 116.6_{sp}, 116.4_{ap}(C-3‴, C-5‴), 113.8 (C-2′, C-6′), 112.4 (C-3a), 14.9_{sp}, 13.6_{ap} (CH_3). MS (EI^+): *m/z* 483(M+, 100%), 485 (M + 2, 46), 362(49), 346 (94), 318 (89), 277 (14), 242 (32).

N′-(2-Chlorobenzylidene)-6-(4-chlorophenyl)-3-methyl-1-phenyl-1*H*-pyrazolo[3,4-b]pyridine-4-carbohydrazide (**2k**) Compound **2k** was prepared by the reaction of **1** with 2-chlorobenzaldehyde. The yellow product was recrystallized from ethanol. Yield: 75%. m.p 212–214 °C; IR ν_{max} (cm^{-1}): 3188(N–H); 3054 (CH-Ar); 2900 (CH-Aliph); 1654 (C=O); 1607, 1593 (C=C); 691 (C–Cl). ^{1}H NMR (500 MHz, DMSO-d_6): $\delta = 12.57_{(sp+ap)}$ (s, 1H, NH), 8.86_{sp}, 8.57_{ap} (2 s, 1H, N=CH) 8.36 (d, $J = 8.0$ Hz, 2H, H-2″, H-6″), $8.32_{(sp+ap)}$ (d, $J = 8.0$ Hz, 2H, H-2′, H-6′), 8.21_{sp}, 8.05_{ap} (2 s, 1H, H-5), $8.11–8.13_{(sp+ap)}$ (d, $J = 7.6$ Hz, 1H, H-6‴) $7.74–7.43_{(sp+ap)}$ (m, 6H, H-3′, H-5′, H-3″ H-5″, H-3‴, H-4‴), 7.38_{sp}, 7.32_{ap} (t, $J = 7.0$ Hz, 1H, H-4′), $2.63_{(sp+ap)}$ (s, 3H, CH_3). Rotamers percentage $sp_{(75\%)}$: $ap_{(25\%)}$. ^{13}C NMR (125 MHz, DMSO-d_6): $\delta = 167.5_{sp}$, 162.1_{ap} (C=O), 155.5(C-6), 151.4 (C-7a), 145.5 (N=CH), 142.7 (C-3), 139.3 (C-4), 138.9 (C-1′), 137.2 (C-1″), 135.6 (C-1‴), 133.9 (C-2‴), 132.4 (C-4″), 132.2_{sp}, 132.1_{ap}, (C-4‴), 131.6_{sp},130.5_{ap}(C-3‴), 129.8 (C-3″, C-5″), 129.7 (C-3′, C-5′), 129.6 (C-6‴), 129.1 (C-2″, C-6″), 128.2 (C-3‴, C-5‴), 127.6 (C-4′), 126.4 (C-5), 121.2_{sp},120.9_{ap}(C-2′, C-6′),113.9 (C-3a), 15.0_{ap}, 14.4_{sp} (CH_3). MS (EI^+): *m/z* 499 (M+, 100%), 501 (M + 2, 64), 503 (M + 4, 13), 362 (37), 346 (93), 318 (69), 277 (8), 242 (27).

N′-(3-Chlorobenzylidene)-6-(4-chlorophenyl)-3-methyl-1-phenyl-1*H*-pyrazolo[3,4-b]pyridine-4-carbohydrazide (**2l**) Compound **2l** was prepared by the reaction of **1** with 3-chlorobenzaldehyde. The yellow product was recrystallized from ethanol. Yield: 60%. m.p 246–247 °C; IR ν_{max} (cm^{-1}): 3178 (N–H); 3051 (CH-Ar); 2923 (CH-Aliph); 1656 (C=O); 1595; 1572; 1506 (C=C); 683 (C–Cl). ^{1}H NMR (500 MHz, DMSO-d_6): $\delta = 12.56_{ap}$, 12.42_{sp} (2s, 1H, NH), $8.40_{(sp+ap)}$ (s, 1H, N=CH), $8.34_{(sp+ap)}$ (d, $J = 8.6$ Hz, 2H, H-2″, H-6″), $8.31_{(sp+ap)}$ (d, $J = 7.8$ Hz, 2H, H-2′, H-6′), 8.17_{sp}, 8.04_{ap} (2 s, 1H, H-5), $7.86_{(sp+ap)}$ (s, 1H, H-2‴), $7.77_{(sp+ap)}$ (d, J = 6.4 Hz, 1H, H-6‴), $7.66_{(sp+ap)}$ (d, $J = 8.6$ Hz, 2H, H-3″, H-5″), $7.62_{(sp+ap)}$ (t, $J = 7.5$ Hz, 2H, H-3′, H-5′), $7.54_{(sp+ap)}$ (m,1H, H-4‴), $7.38_{(sp+ap)}$ (t, $J = 7.3$ Hz, 1H, H-5‴), $7.34–7.23_{(sp+ap)}$ (m, 1H, H-4′), $2.62_{(sp+ap)}$ (s, 3H, CH_3). Rotamers percentage $sp_{(78\%)}$: $ap_{(22\%)}$. ^{13}C NMR (125 MHz, DMSO-d_6): $\delta = 167.5_{sp}$, 162.2_{ap} (C=O), 155.4 (C-6), 151.4 (C-7a), 147.9 (N=CH), 142.7 (C-3), 139.4 (C-4), 139.3 (C-1′), 139.0 (C-1″), 137.0 (C-1‴), 136.6 (C-3‴), 135.6 (C-5‴), 134.2 (C-C-4″), 130.6 (C-4‴), 129.8 (C-3″, C-5″), 129.7 (C-6‴), 129.6 (C-2‴), 129.6 (C-2″, C-6″), 127.1 (C-3″, C-5″),

126.5 (C-4′), 126.4 (C-5), 121.2 (C-2′, C-6′), 113.8 (C-3a), 14.9_{ap}, 13.7_{sp} (CH_3). MS (EI^+): *m/z* 499 (M+, 88%), 501 (M + 2, 77), 503 (M + 4, 13), 362 (48), 346 (100), 318 (58), 277 (20), 242 (31).

N′-(4-Chlorobenzylidene)-6-(4-chlorophenyl)-3-methyl-1-phenyl-1*H*-pyrazolo[3,4-b]pyridine-4-carbohydrazide (**2m**) Compound **2m** was prepared by the reaction of **1** with 4-chlorobenzaldehyde. The yellow product was recrystallized from ethanol. Yield: 63%. m.p 285–287 °C; IR ν_{max} (cm^{-1}): 3188 (N–H); 3057 (CH-Ar); 2928 (CH-Aliph); 1656 (C=O); 1595; 1548; 1560 (C=C); 690 (C–Cl). ^{1}H NMR (500 MHz, DMSO-d_6): $\delta = 12.50_{ap}$, 12.31_{sp} (2 s, 1H, NH), 8.41_{sp}, 8.36_{ap} (2 s, 1H, N=CH), $8.34_{(sp+ap)}$ (d, $J = 8.6$ Hz, 2H, H-2″, H-6′′), $8.31_{(sp+ap)}$ (d, $J = 8.2$ Hz, 2H, H-2′, H-6′), 8.16_{sp}, 8.03_{ap} (2 s, 1H, H-5) $7.83_{(sp+ap)}$ (d, $J = 8.5$ Hz, 2H, H-2‴,H-6‴), $7.67_{(sp+ap)}$ (d, $J = 8.6$ Hz, 2H, H-3″, H-5″), $7.62_{(sp+ap)}$ (t, $J = 8.4$ Hz, 2H, H-3′, H-5′), $7.57_{(sp+ap)}$ (t, $J = 8.5$ Hz, 2H, H-3‴, H-5‴), $7.38_{(sp+ap)}$ (t, $J = 7.3$ Hz, 1H, H-4′), $2.62_{(sp+ap)}$ (s, 3H, CH_3). Rotamers percentage $sp_{(73\%)}$: $ap_{(27\%)}$. ^{13}C NMR (125 MHz, DMSO-d_6): $\delta = 168.0_{ap}$, 162.1_{sp} (C=O), 155.4 (C-6), 151.4 (C-7a), 148.2 (N=CH), 145.1 (C-3), 142.7 (C-4), 139.3 (C-4‴), 139.1 (C-1′), 137.0 (C-1″), 135.6 (C-4″), 135.5_{ap}, 133.3_{sp} (C-1‴), 129.8 (C-2‴, C-6‴), 129.7 (C-3″, C-5″), 129.6 (C-3′, C-5′), 129.5 (C-3‴, C-5‴), 129.5 (C-2″, C-6″), 126.4 (C-4′), 121.2 (C-2′, C-6′), 120.9 (C-5), 113.8 (C-3a), 14.9_{sp}, 13.6_{ap} (CH_3). MS (EI^+): *m/z* 499 (M+, 100%), 501 (M + 2, 62), 503 (M + 4, 16), 362 (45), 346 (79), 318 (63), 277 (8), 242 (30).

N′-(2-Methoxybenzylidene)-6-(4-chlorophenyl)-3-methyl-1-phenyl-1*H*-pyrazolo[3,4-b]pyridine-4-carbohydrazide (**2n**) Compound **2n** was prepared by the reaction of **1** with 2-methoxybenzaldehyde. The yellow product was recrystallized from ethanol. Yield: 77%. m.p 229–231 °C; IR ν_{max} (cm^{-1}): 3, 156 (N–H); 3006 (CH-Ar); 2940 (CH-Aliph); 1648 (C=O); 1598; 1561; 1491 (C=C); 688 (C–Cl). ^{1}H NMR (500 MHz, DMSO-d_6): $\delta = 12.38_{ap}$, 12.23_{sp} (2 s, 1H, NH), 8.78_{sp}, 8.50_{ap} (2 s, 1H, N=CH), $8.36_{(sp+ap)}$ (d, $J = 7.8$ Hz, 2H, H-2″, H-6″), $8.32_{(sp+ap)}$ (d, $J = 7.8$ Hz, 2H, H-2′, H-6′), 8.17_{sp}, 8.02_{ap} (2 s, 1H, H-5), $7.96_{(sp+ap)}$ (d, $J = 7.5$ Hz, 1H, H-6‴), $7.67_{(sp+ap)}$ (d, $J = 8.2$ Hz, 2H, H-3″, H-5″), $7.62_{(sp+ap)}$ (t, $J = 7.4$ Hz, 2H, H-3′, H-5′) 7.52–$7.35_{(sp+ap)}$ (m, 2H, H-4‴, H-4′), 7.15–$7.08_{(sp+ap)}$ (m, 2H, H-5‴, H-3‴), 6.73_{ap} (t, $J = 1$H, H-5_{ap}‴) 3.88_{sp}, 3.82_{ap} (2 s, 3H, OCH_3), $2.63_{(sp+ap)}$ (s, 3H, CH_3). Rotamers percentage $sp_{(76\%)}$: $ap_{(24\%)}$. MS (EI^+): *m/z* 495 (M+, 81%), 497 (M + 2, 29), 464 (6), 362 (100), 346 (24), 318 (53), 277 (10), 242 (24).

N′-(4-Methoxybenzylidene)-6-(4-chlorophenyl)-3-methyl-1-phenyl-1*H*-pyrazolo[3,4-b]pyridine-4-carbohydrazide (**2o**) Compound **2o** was prepared by the reaction of **1** with 4-methoxybenzaldehyde. The yellow product was recrystallized from ethanol. Yield: 73%. m.p 280–283 °C; IR ν_{max} (cm^{-1}): 3197 (N–H); 3066 (CH-Ar); 2966 (CH-Aliph); 1654 (C=O); 1596; 1572; 1507(C=C); 689 (C–Cl). ^{1}H NMR (500 MHz, DMSO-d_6): $\delta = 12.31_{ap}$, 12.14_{sp} (2 s, 1H, NH), 8.63_{ap}, 8.37_{sp}(2 s, 1H, N=CH) $8.34_{(sp+ap)}$ (d, $J = 8.0$ Hz, 2H, H-2″, H-6″), $8.32_{(sp+ap)}$ (d, $J = 8$ Hz, 2H, H-2′, H-6′), 8.15_{sp}, 8.01_{ap}(2 s, 1H, H-5), 7.82_{ap}, 7.75_{sp} (d, $J = 8.6$ Hz, 2H, H-2‴, H-6‴), $7.67_{(sp+ap)}$ (d, $J = 8$ Hz, 2H, H-3″, H-5″), $7.62_{(sp+ap)}$ (t, $J = 8.1$ Hz, 2H, H-2′, H-5′), $7.38_{(sp+ap)}$ (t, $J = 7.0$ Hz, 1H, H-4′), 7.27, $6.84_{(sp+ap)}$ (m, 2H, H-3‴, H-5‴), 3.84_{sp}, 3.68_{ap} (2s, 3H, OCH_3), $2.62_{(sp+ap)}$ (s, 3H, CH_3). Rotamers percentage $sp_{(75\%)}$: $ap_{(25\%)}$. ^{13}C NMR (125 MHz DMSO-d_6): $\delta = 172_{ap}$, 161.8_{sp} (C=O), 161.7 (C-4‴), 155.5 (C-6), 151.4 (C-7a), 149.4 (N=CH), 142.8 (C-3), 139.5 (C-4), 139.3 (C-4″), 137.1 (C-1′), 135.6 (C-1″), 129.8 (C-1‴), 129.7 (C-3″, C-5″), 129.6 (C-3′, C-5′), 129.5 (C-2‴, C-6‴), 128.7 (C-2″, C-6″), 127.2 (C-4′), 126.2 (H-5), 121.2 (C-2′, C-6′), 114.9 (C-3‴, C-5‴), 113.4 (C-3a), 55.8_{sp},55.7_{ap} (OCH_3), 14.9_{sp}, 13.6_{ap} (CH_3). MS (EI^+): *m/z* 495 (M+, 86%), 497 (M + 2, 38), 464 (4), 362 (100), 346 (26), 318 (59), 277 (10), 242 (22).

N′-(2-Hydroxy-3-methoxybenzylidene)-6-(4-chlorophenyl)-3-methyl-1-phenyl-1*H*-pyrazolo[3,4-b]pyridine-4-carbohydrazide (**2p**) Compound **2p** was prepared by the reaction of **1** with 2-hydroxy-3-methoxybenzaldehyde. The yellow product was recrystallized from ethanol. Yield: 68%. m.p 215–217 °C; IR ν_{max} (cm^{-1}): 3393 (OH); 3006 (CH-Ar); 2920 (CH-Aliph); 1654 (C=O); 706 (C–Cl). ^{1}H NMR (500 MHz, DMSO-d_6): $\delta = 10.88_{ap}$, 10.70_{sp} (2 s, 1H, NH), 10.19_{sp}, 8.99_{ap} (2 s, 1H, N=CH), $8.30_{(sp+ap)}$ (d, $J = 7.9$ Hz, 2H, H-2″, H-6″), $8.28_{(sp+ap)}$ (d, $J = 8.5$ Hz, 2H, H-2′, H-6′), 7.94_{sp}, 7.33_{ap} (2 s, 1H, H-5), $7.66_{(sp+ap)}$ (d, $J = 8.4$ Hz, 2H, H-3″, H-5″), $7.61_{(sp+ap)}$ (t, $J = 7.8$ Hz, 2H, H-3′, H-5′), 7.40–7.26 (m, 2H, H-4′, H-6‴), 7.13_{sp}, 7.08_{ap} (d, $J = 7.9$ Hz, 1H, H-4‴), $6.91_{(sp+ap)}$ (t, $J = 7.9$ Hz, 1H, H - 5‴), $3.61_{(sp+ap)}$ (s, 3H, OCH_3) $2.61_{(sp+ap)}$ (s, 3H, CH_3). Rotamers percentage $sp_{(70\%)}$: $ap_{(30\%)}$. ^{13}C NMR (125 MHz, DMSO-d_6): $\delta = 168_{sp}$, 164.9_{ap} (C=O), 163.2 (C-2‴), 155.3 (C-6), 151.4 (C-7a), 149.0 (N=CH), 148.4 (C-3‴), 142.9 (C-3), 139.3 (C-4), 138.9 (C-1′), 137.1 (C-1″), 135.5 (C-4″), 130.5 (C-6‴), 129.7 (C-3″, C-5″), 129.6 (C-3′, -5′), 129.6 (C-2″, C-6″), 126.3 (C-4′), 122.5 (C-5), 121.1 (C-2′, C-6′), 120.1 (C-6‴), 119.8 (C-4‴), 118.7 (C-5‴), 113.4 (C-3a),56.4 (OCH_3), 14.9 (CH_3). MS (EI^+): m/z 511 (M+, 80%), 513 (M + 2,), 419 (80), 362 (26), 346 (100), 318 (81), 277 (12), 242 (24).

N′-(3-Hydroxybenzylidene)-6-(4-chlorophenyl)-3-methyl-1-phenyl-1*H*-pyrazolo[3,4-b]pyridine-4-carbohydrazide (**2q**) Compound **2q** was prepared by the reaction of **1** with 3-hydroxybenzaldehyde. The yellow product was recrystallized from ethanol. Yield: 39%. m.p 290–292 °C; IR ν_{max}

(cm^{-1}): 3394 (OH); 3043 (CH-Ar); 2963 (CH-Aliph); 1650 (C=O); 689 (Cl). ^{1}H NMR (500 MHz, DMSO-d_6): $\delta =$ 12.36_{ap}, 12.21_{sp} (2 s, IH, NH), 8.51_{ap}, 8.35_{sp} (2 s, 1H, N=CH), $8.33_{(sp+ap)}$ (d, $J = 6.2$ Hz, 2H, H-2″, H-6″), $8.30_{(sp+ap)}$ (d, $J = 10$ Hz, 2H, H-2′, H-6′), 8.14_{sp}, 8.06_{ap} (2 s, 1H, H-5), 7.99_{sp},7.93_{ap} (2 s, 1H, OH), $7.69–7.59_{(sp+ap)}$ (m, 5H, H-3″, H-5″, H-3′, H-5′, H-2‴), 7.42-$7.26_{(sp+ap)}$ (m, 3H, H-4″, H-4′, H-6″, H-5‴), $2.61_{(sp+ap)}$ (s, 3H, CH_3). Rotamers percentage $sp_{(76\%)}$:$ap_{(24\%)}$. ^{13}C NMR (125 MHz, DMSO-d_6): $\delta = 161.9$ (C=O), 155.5 (C-3‴), 151.7 (C-6), 150.7 (C-7a), 149.5 (N=CH), 146.2 (C-3), 139.3 (C-4), 139.2 (C-4″) 139.1 (C-1′), 137.0 (C-1‴), 135.6 (C-1″), 135.4 (C-4′), 129.8 (C-3″, C-5″), 129.7 (C-2″, C-6″), 129.6 (C-3′, C-5′), 126.5 (C-5), 121.2 (C-2′, C-6′), 120.1 (C-6‴), 115.1 (C-2‴), 113.3 (C-5‴), 112.9 (C-3a), 112.2 (C-4‴), 14.8_{sp}, 13.6_{ap}(CH_3). MS (EI^+): *m/z* 481 (M+, 78%), 483 (M + 2, 30), 419 (58), 362 (55), 346 (100), 318 (27.7), 242 (33).

N′-(4-Hydroxybenzylidene)-6-(4-chlorophenyl)-3-methyl-1-phenyl-1*H*-pyrazolo[3,4-b]pyridine-4-carbohydrazide (**2r**) Compound **2r** was prepared by the reaction of **1** with 4-hydroxybenzaldehyde. The yellow product was recrystallized from ethanol. Yield: 75%. m.p ›300 °C; Lit. (Dias et al. 2007) [›310 °C]. IR ν_{max} (cm^{-1}): 3313 (OH); 3199 (CH-Ar); 3097 (CH-Aliph); 1647 (C=O); 692 (C–Cl).

N′-(4-(Dimethylamino)benzylidene)-6-(4-chlorophenyl)-3-methyl-1-phenyl-1*H*-pyrazolo[3,4-b]pyridine-4-carbohydrazide (**2s**) Compound **2s** was prepared by the reaction of **1** with 4-dimethylaminobenzaldehyde. The yellow product was recrystallized from ethanol. Yield: 98%. m.p 214–215 °C; Lit. (Geraldo et al. 2010) [212 °C]; IR (ν-cm^{-1}): 3192 (N–H); 1696 (C=O). MS (EI^+): *m/z* 499 (M+, 1%), 501 (M + 2, 34), 419 (84), 377 (21), 362 (13), 346 (100), 318 (74), 277 (12), 242 (20).

N′-(Furan-2-yl-methylene)-6-(4-chlorophenyl)-3-methyl-1-phenyl-1*H*-pyrazolo[3,4-b]pyridine-4-carbohydrazide (**2t**) Compound **2t** was prepared by the reaction of **1** with furan-2-carbaldehyde. The yellow product was recrystallized from ethanol. Yield: 60%. m.p 250–252 °C; IR: ν_{max} (cm^{-1}): 3175 (N–H); 3011 (CH-Ar); 2944 (CH-Aliph); 1652; 1600; 1559 (C=O). ^{1}H NMR (500 MHz, DMSO-d_6): $\delta = 12.36_{ap}$, 12.22_{sp} (2s, 1H, NH), 8.51_{ap}, 8.34_{sp} (2 s, 1H, N=CH), $8.32_{(sp+ap)}$ (d, $J = 7$ Hz, 2H, H-2″, H-6″), $8.30_{(sp+ap)}$ (d, $J = 6.2$ Hz, 2H, H-2′, H-6′), 8.14_{sp}, 8.06_{ap} (2 s, 1H, H-5), 7.99_{ap}, 7.92_{sp} (2s, 1H, H-3‴), $7.66_{(sp+ap)}$ (d, $J = 8.6$ Hz, 2H, H-3″, H-5″), 7.6 (t, $J = 7.9$ Hz, 2H, H-3′, H-5′), $7.38_{(sp+ap)}$ (t, $J = 7.2$ Hz, 1H, H-4′), 7.03_{sp}, 6.77_{ap} (d, $J =$ 3.3 Hz, 2H, H-4‴, H-5‴), 2. $62_{(sp+ap)}$ (s, 3H, CH_3). Rotamers percentage $sp_{(75\%)}$: $ap_{(25\%)}$. ^{13}C NMR (125 MHz, DMSO-d_6): $\delta = 167.8_{ap}$, 161.9_{sp} (C=O), 155.4 (C-6), 151.4 (C-7a), 149.5 (C-1‴), 146.2 (C-3‴), 142.7 (C-3), 139.3 (C-4), 139.2 (N=CH), 139.1 (C-1′), 137.0 (C-1″), 135.6 (C-4″), 129.8 (C-3″, C-5″), 129.7 (C-3′, C-5′), 129.6 (C-2″, C-6″), 126.4 (C-4′), 121.1 (C-2′, C-6′), 120.9 (C-5), 115.0 (C-5‴), 113.7 (C-4‴), 112.8_{ap}, 112.3_{sp} (C-3a), 14.9_{sp}, 13.6_{ap} (CH_3). MS (EI^+): *m/z* 455 (M+, 100%), 457 (M + 2, 40), 346 (75), 318 (67), 277 (14), 242 (26).

Molecular docking studies

Protein (Receptor) structure preparation

In order to understand the insight mechanism of binding mode of synthesized compound with receptor residues molecular docking simulations were performed for compounds (**2a–2t** and Aspirin). Molecular docking studies were performed by using MOE 2009.10 (Ahad et al. 2015; Ahmad et al. 2015; Ahmad et al. 2015). The human PGH-2 synthase 3D model of COX-1 (PDB-ID: 1Q4G) and COX-2 (PDB-ID: 3NT1) were retrieved from PDB (source www.rcsb.org//pdb/). The molecular modeling and computational research is also widely used in literature for drug designing (Karmakar and Singh 2017; Li et al. 2014; Srikala et al. 2017).

AMBER99 force field function of MOE was used for 3D protonation and energy minimization by receptor molecule optimization. The slope was set at 0.5 and receptor was reduced till its root mean square slope reached below point 0.05. After 3D protonation of receptor protein and hide molecule option was used to hydrogen molecule. Again MOE option of surface and map was used for pinpointing the pocket residues and docking site. This 3D protonated and energy minimized receptor molecules were used for molecular docking analysis.

Ligands preparation and database construction

The scaffolds of synthesized compounds (**2a–2t** and Aspirin) were constructed by using chem3D pro 12.0. Their 3D structures were then saved in .mol file for docking analysis. The ligands structure prepared by addition of hydrogen atom and energy minimization at 0.05 gradients was done with the help of MMFF94X force field option in MOE. These ligands were then added into a database and were used for docking against the targeted receptor protein.

Molecular docking analysis

Molecular docking analysis was executed after receptor protein and ligands molecule preparation. The .mbd format was used for saving the docking output database file

containing receptor ligand complexes. In order to evaluate the ligands interactions with receptor protein active sites residue, complexes with minimum *S* values were taken. MOE ligX option was used for analysis of best docked pose having highest negative binding energy value (*S* value), highest hydrogen bonding, and π–π interactions.

Biological activities

Antiplatelet activity

Antiplatelet activity against AA and collagen was determined on human whole blood as previously described method along with slight modifications (Storey et al. 1998). Blood (5 mL) was drawn from healthy volunteer by careful venipuncture (after getting their consents), poured into trisodium citrate (0.5 mL; 3.8%) containing falcon tube. The tube with blood was then incubated at 37 °C for 30 min. The aliquots (460 µL) of this pre-incubated blood was mixed with 600 µL fixing solution (0.5% formaldehyde in PBS) to take the baseline platelet count at $t = 0$ min. In a separate tube, 20 µL of antagonist, i.e., DMSO/Aspirin/compounds (**2a–2t**) were dispensed in falcon containing 460 µL whole blood and stirred for 2 min at 37 °C. Platelet count was recorded after 6 min on platelet counter (Sysmex XT-1800i) after adding and mixing 20 µL of agonist, i.e., AA/collagen. Aspirin was used as a control while percentage inhibition was calculated by the following formula. All assays were completed within 90 min of venipuncture.

Percentage inhibition = (Agonist platelet count/Baseline platelet count) × 100

Percentage aggregation = [(Baseline platelet count − Agonist platelet count)/Baseline platelet count] × 100

(Where baseline platelet count is the first blood draw count at $t = 0$ min).

Antioxidant activity

2,2-Diphenyl-1-picrylhydrazyl (DPPH) anti-oxidant activity

Free radical scavenging effect of synthesized compounds was determined with DPPH assay (Baylac and Racine 2003). Different concentrations (1 and 8 mM, 10 µL) of compounds in respective solvents were mixed with DPPH (100 µM, 90 µL) with total volume of 100 µL in 96-well plates. This reaction mixture was incubated at 37 °C for 30 min. Microplate reader (BIO RAD Model 680) was used to record the absorbance of resulting reaction mixture at 517 nm. Experiments were performed in triplicate while trolox was used as standard antioxidant. The decrease in absorbance showed increased level of radical scavenging activity which was determined by following formula.

$$\text{Percent scavenging activity} = [1 - (\text{Abs of test compound}/\text{Abs of control})] \times 100$$

ABTS antioxidant activity

2,2′-azino-bis(3-ethylbenzothiazoline-6-sulfonic acid (ABTS) antioxidant activity was also performed in the same way as for DPPH. Whereas, ABTS (7 mM) solution was prepared by mixing it with potassium persulfate (2.45 M, 2.6 mL) solution. The resulting solution was incubated for 12–16 h in dark. Greenish blue solution obtained was diluted with ethanol to give the 0.7 absorbance at 734 nm. All the samples were run in triplicates. Trolox was used as standard drug.

Iron (Fe^{2+}) chelating activity

Iron (Fe^{2+}) chelating activity was performed by the previously reported method with slight modifications (Narsinghani et al. 2013). A volume of 40 µL of sample was incubated with 40 µL ferric chloride (200 µM) and 20 µL of *o*-phenanthroline solution (0.05%) at room temperature for 10 min. Absorbance was measured at 510 nm and trolox was taken as standard.

Results and discussion

Characterization: ^{1}H and ^{13}C NMR spectra

The synthesis of new *N*′-benzylidene-3-methyl-1-phenyl-6-*p*-chlorophenyl-1*H*-pyrazolo[3,4-*b*]pyridine-4-carbohydrazide (**2a–2t**) was carried out in five steps as shown in Scheme 1. Condensation of 3-aminocrotonitrile with phenyl hydrazine gave 5-amino-3-methyl-1-phenyl-1*H*-pyrazole which on reaction with *p*-chlorobenzaldehyde followed by ethyl pyruvate afforded ethyl 6-*p*-chlorophenyl-3-methyl-1-phenyl-1*H*-pyrazolo[3,4-*b*]pyridine-4-carboxylate. The ester treated with hydrazine monohydrate yielded 6-*p*-chlorophenyl-3-methyl-1-phenyl-1*H*-pyrazolo[3,4-*b*]pyridine-4-carbohydrazide (**1**) and finally *N*′-(arylmethylidene)-3-methyl-1-phenyl-6-*p*-chlorophenyl-1*H*-pyrazolo[3,4-*b*]pyridine-4-carbohydrazides (**2a–2t**) were prepared from the condensation of **1** with various aromatic aldehydes in glacial acetic acid in 25–98% yield (Supporting Supplementary Table S1).

Structure elucidation of synthesized compounds (**2a–2t**) was determined using different spectroscopic techniques such as FT-IR, ^{1}H NMR, ^{13}C NMR and EI-MS spectral

Scheme 1 Synthesis of the target *N′*-benzylidene-3-methyl-1-phenyl-6-*p*-chlorophenyl-1*H*-pyrazolo[3,4-*b*]pyridine-4-carbohydrazides (**2a-2t**)

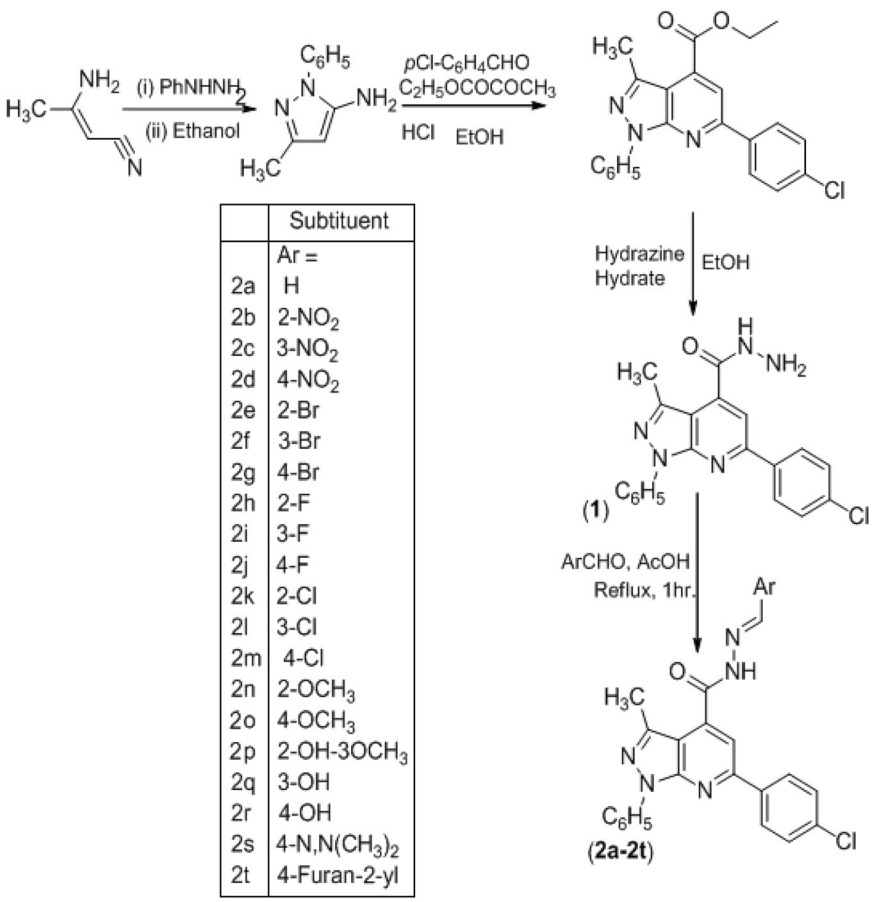

	Subtituent
	Ar =
2a	H
2b	2-NO_2
2c	3-NO_2
2d	4-NO_2
2e	2-Br
2f	3-Br
2g	4-Br
2h	2-F
2i	3-F
2j	4-F
2k	2-Cl
2l	3-Cl
2m	4-Cl
2n	2-OCH_3
2o	4-OCH_3
2p	2-OH-3OCH_3
2q	3-OH
2r	4-OH
2s	4-N,N(CH_3)$_2$
2t	4-Furan-2-yl

data. The reaction was checked by TLC and purity of compounds was entrenched from sharp melting points. Assignment of specific characteristic IR bands furnished the important indications for formation of (**2a–2t**). FT-IR spectra of synthesized compounds displayed their characteristics stretching vibration in the range 3150–3300 cm^{-1} for NH and 1648–1680 cm^{-1} for C=O. ^{1}H NMR spectra of synthesized compounds showed characteristics signals in the expected regions; 2.62–2.63 ppm for CH_3 and 12–13 ppm for NH along the aromatic proton in the respective region. The ^{13}C NMR clearly showed a CH_3 region in 13–14 ppm.

In ^{1}H NMR of compounds (**2a–2p, 2t**), duplicate appearance of signals were observed for NH, N=CH, H-5, CH_3 and aryl protons. It has already been reported in literature that acyl hydrazones normally exist as isomeric mixture (Koop et al. 2001; G Palla et al. 1982). Depending on the arrangement of the group around C=N as well as around N–N and C(O)–N bond, different conformers may exist (Fig. 1) (Fraser et al. 1981; Uwe Himmelreich et al. 1990; U Himmelreich et al. 1993; Gerardo Palla et al. 1986; Elzbieta Wyrzykiewicz et al. 2000). Z(N–N) (**V–VIII**, Fig. 1) conformations could not be realized due to steric repulsion between aroyl group and benzylidene moieties.

Steric factor also minimized the possibility of Z(>C=N) geometric isomers (**III–IV**, Fig. 1). It has been claimed by the researcher on the basis of X-Ray data that acyl hydrazone exist only in E(>C=N) geometrical isomers (i.e., **I** and **II**, Fig. 1), their further study confirmed that the duplicate signals in acyl hydrazones are due to amide conformers [sp ($E_{C=N}$, E_{N-N}) (**I**) and **ap**($E_{C=N}$, E_{N-N}) (**II**)(Fig. 1) (Glidewell et al. 2004a, 2004b; E Wyrzykiewicz and Prukala 1998).

Similar conclusions have also been drawn by many authors utilizing the different NMR techniques (Nakka et al. 2010; Patorski et al. 2012; Syakaev et al. 2006). The duplicate appearance of signals have been observed in the NMR spectra of *N′*-(arylmethylidene)-6-*p*-chlorophenyl-3-methyl-1-phenyl-1*H*-pyrazol[3,4-*b*]pyridine-4-carbohydrazide (**2a–2p, 2t**), the intensities of duplicate signal confirmed the existence of syn-periplanar (**sp**) conformers as major component as compared to anti-pariplanar (**ap**) conformers due to less steric hindrance of attached moieties in case of **sp** conformers (Supporting Supplementary Fig. S1) (Gerardo Palla et al. 1986). The assignment of the signals for **sp** and **ap** conformers is indicated in Supporting Supplementary Tables S2, S3.

The NH proton in **ap** conformer of acylhydrazones (**2a–2p, 2t**) appeared downfield to that of NH proton in **sp**

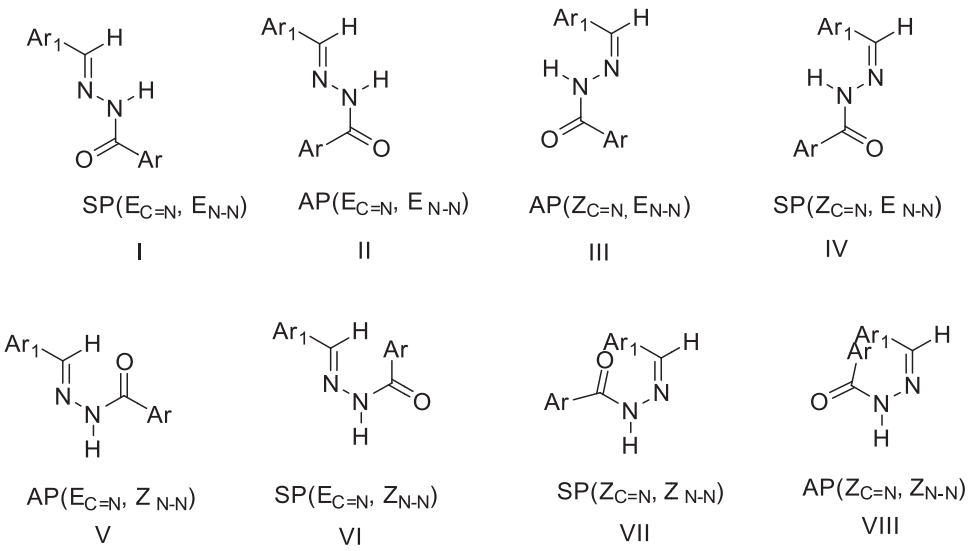

Fig. 1 Eight possible (E and Z) conformer of acyl-hydrazones

conformers. It can be attributed to the close proximity of >C=O in **ap** isomer, which may exert field and anisotropic effect. The N=CH proton in **sp** conformers appeared down field to that of N=CH proton in E_{ap} isomer in most of the cases probably due to electronic effect (inductive effect, field effect, and anisotropic effect) of nearby moieties. The same behavior had already been reported in literature (Syakaev et al. 2006).

The signals for H-5 proton in **sp** was appeared downfield due to anisotropic effect of >C=O moiety which seems to be lessen in **ap** due to distortions in structure planes as a result of torsional strain of nearby groups. By the similar reasons, the CH_3 group in **sp** conformers appeared on downfield as compared to the CH_3 in **ap** (which in most of the cases is overlapped by residual DMSO signals). The chemical shift of phenyl protons of benzylidene moiety have been found to be affected by the existence of **sp/ap** conformations. The presence of carbon signals more than the expected indicate the presence of conformational mixture (Bock and Pedersen 1974). The ^{1}H and ^{13}C NMR spectra have been recorded in DMSO-d_6. Appearance of double signals, confirmed the formation of **sp/ap** conformations (Supporting Supplementary Fig. S3). Accompanying NMR, the compounds (**2a–2t**) were subjected to ESI-MS analysis for detecting the molecular mass and confirmation of synthesized compounds. Results obtained for structure elucidation of all the synthesized compounds (**2a–2t**) provided solid and strong affirmation and endorsement for the complete synthesis of target compounds.

Biological activity

DPPH, ABTS, iron chelating and antiplatelet activity assays were used to evaluate the antioxidant and antiplatelet activity of *N*′-arylmethylidene-3-methyl-1-phenyl-6-chlorophenyl-1*H*-pyrazolo[3,4-*b*]pyridine-4-carbohydrazides (**2a–2t**). It has been found that all the compounds exhibited high antioxidant potential except of **2c**, **2f**, and **2t** because of readily available methyl proton which may scavenge the ABTS, DPPH, and Fe free radical. Results are tabulated in Supporting Supplementary Table S4.

The antiplatelet activity has been displayed by all the compounds but (**2c**, **2e**, **2f**, **2g**, **2i**, **2m**, **2o** and **2q**) have revealed superlative antiplatelet activity. All the results were summarized in Table 1.

Molecular docking studies

Finding interactive residues in COX-1 and COX-2

The main focus of the present work was sorting of most potent compound for antiplatelet activity from the series (**2a–2t**) via Molecular Dockings and computational screening with targeted protein. The docked compounds (**2o 2c, 2e, 2f, 2g, 2l, 2i, 2m, 2o, 2q, 2s** and Aspirin) showed the binding interaction with the pocket residues. Present work also showed that 11 compounds out of 20 compounds involved in the hydrogen bond formation with the interacting residues for antiplatelet activity against (COX-1 and COX-2) (Fig. 2a, b). Thus these synthesized compounds (**2a–2t**) can be considered potent antiplatelet drugs and further be used with diverse approaches including pharmacological and drug designing (Table 2a, b).

Computational detail

To understand the radical scavenging procedure H-atom transfer, and one-electron transfer mechanisms are frequently used (Belcastro et al. 2006; Wright et al. 2001). Usually, H-atom transfer mechanism is used to understand

Table 1 Antiplatelet activity results of synthesized compounds (**2a–2t**)

Compound no.	R group	AA (100 μM)		Collagen (5 μg/mL)	
		% Inhibition	% Inhibition	% Aggregation	% Inhibition
2a	H	73.47 ± 2.6	26.53 ± 2.8	73.47 ± 2.6	26.52 ± 2.4
2b	$2NO_2$	72.60 ± 2.7	51.16 ± 1.9	74.22 ± 2.2	25.77 ± 1.8
2c	$3NO_2$	86.54 ± 2.1	13.45 ± 0.29	79.81 ± 3.9	20.18 ± 2.1
2d	$4NO_2$	73.33 ± 3.3	26.66 ± 2.7	78.26 ± 0.7	21.73 ± 1.3
2e	2Br	78.94 ± 3.7	21.05 ± 2.3	73.68 ± 2.1	26.31 ± 1.9
2f	3Br	70.12 ± 25	29.87 ± 0.5	74.26 ± 0.1	25.73 ± 1.9
2g	4Br	70.12 ± 1.5	29.87 ± 2.5	75.14 ± 2.1	24.85 ± 3.1
2h	2F	76.44 ± 2.4	23.55 ± 2.6	88.44 ± 1.4	11.55 ± 1.6
2i	3F	68.59 ± 2.6	31.40 ± 2.4	73.68 ± 2.1	26.31 ± 1.9
2j	4F	71.64 ± 3.4	28.35 ± 2.6	78.22 ± 2.2	21.77 ± 1.8
2k	2Cl	75.55 ± 2.6	24.44 ± 2.4	54.97 ± 0.6	45.02 ± 2.4
2l	3Cl	75.30 ± 2.8	24.69 ± 1.2	97.07 ± 0.2	2.923 ± 2.7
2m	4Cl	74.08 ± 3.7	25.91 ± 2.3	80.70 ± 2.5	19.29 ± 2.5
2n	$2OCH_3$	70.12 ± 2.5	29.87 ± 0.5	74.45 ± 0.9	23.55 ± 1.2
2o	$4OCH_3$	71.34 ± 4.6	28.65 ± 1.4	83.62 ± 2.3	16.37 ± 2.7
2p	$2OH\text{-}3OCH_3$	80.34 ± 2.3	20.64 ± 3.0	79.82 ± 2.6	20.17 ± 44
2q	3OH	71.11 ± 1.1	28.88 ± 1.9	67.90 ± 0.8	32.10 ± 2.1
2r	4OH	75.55 ± 2.6	24.44 ± 1.4	77.77 ± 1.8	22.22222
2s	$4\text{-}N,N(CH_3)_2$	68.88 ± 1.9	31.11 ± 1.1	83.62 ± 1.3	16.37 ± 2.7
2t	4-Furan-2-yl	77.33 ± 3.3	22.66 ± 2.7	78.66 ± 2.7	21.33 ± 3.3
Aspirin		93.2 ± 1.23	6.81 ± 1.4	94.41 ± 2.01	5.59 ± 2.43

the radical scavenging activity for those compounds which have –OH group. In such compounds, hydrogen atom transfer would be favorable. While the hydrazone derivatives which have been studied in the present work don't have –OH group/groups except **2p–2r**. Thus in the present study, we have shed light on the one-electron transfer mechanism for the hydrazone derivatives. Recently, density functional theory (DFT) has been proved as a proficient method that reproduces the experimental data (Chaudhry et al. 2014; Chaudhry et al. 2014; Irfan and Al-Sehemi 2014). In the present study, ground state geometries have been optimized by adopting the B3LYP functional (Irfan et al. 2016; Irfan et al. 2017) and 6–31G** basis set. The reactivity descriptors have been computed by DFT approach from the Eqs. 1–8. Details about methodology can be found in the reference (Al-Sehemi et al. 2012).

Mulliken electronegativity (χ) was calculated from as:

$$\chi = (E_{\mathrm{HOMO}} + E_{\mathrm{LUMO}})/2 \quad (1)$$

The hardness (η) was computed by using Eq. 2:

$$\eta = (E_{\mathrm{LUMO}} - E_{\mathrm{HOMO}})/2 \quad (2)$$

Electrophilicity (ω) was calculated from the following Eq. 3:

$$\omega = (E_{\mathrm{HOMO}} + E_{\mathrm{LUMO}}/2)^2/2\eta \quad (3)$$

Softness (S) was calculated as:

$$S = 1/2\eta \quad (4)$$

Electrophilicity index (ωi) was calculated from the following equation:

$$\omega i = m^2/2\eta \quad (5)$$

Chemical potential (μ) was calculated from the following equation:

$$\mu = -(\mathrm{HOMO} + \mathrm{LUMO}/2) \quad (6)$$

Ionization potentials (IP) and electron affinities (EA) have been calculated as under

$$\mathrm{IP} = -E_{\mathrm{HOMO}} \quad (7)$$

$$\mathrm{EA} = -E_{\mathrm{LUMO}} \quad (8)$$

All calculations were performed by Gaussian 09 software (Frisch et al. 2009) except QSAR investigations which have been done in Spartan '14 v1.1.8' at B3LYP/6-31G* level which has been proved an efficient and reasonable to interpret the SAR and other physiochemical properties (Al-Sehemi et al. 2017; Al-Sehemi et al. 2016).

Electronic properties

The highest occupied molecular orbitals (HOMOs) and lowest unoccupied molecular orbitals (LUMOs) have been displayed in Fig. 3.The HOMOs are delocalized on the 1-phenyl-1*H*-pyrazolo[3,4-*b*]pyridine moiety in all the studied hydrazone derivatives **2a–2t** except 2 s in which HOMO is delocalized at the (dimethylaminobenzylidene)-hydrazide moiety. In **2a**, **2e–2m**, and **2t**, mainly the LUMOs are localized on the pyrazolo[3,4-*b*]pyridine moiety (benzylidene and phenyl of chlorophenyl), which are also taking part in the formation of LUMOs. The intra-molecular charge transfer (ICT) has been observed from phenyl moiety to the rest of the ring. In **2b–2d**, the LUMO is localized

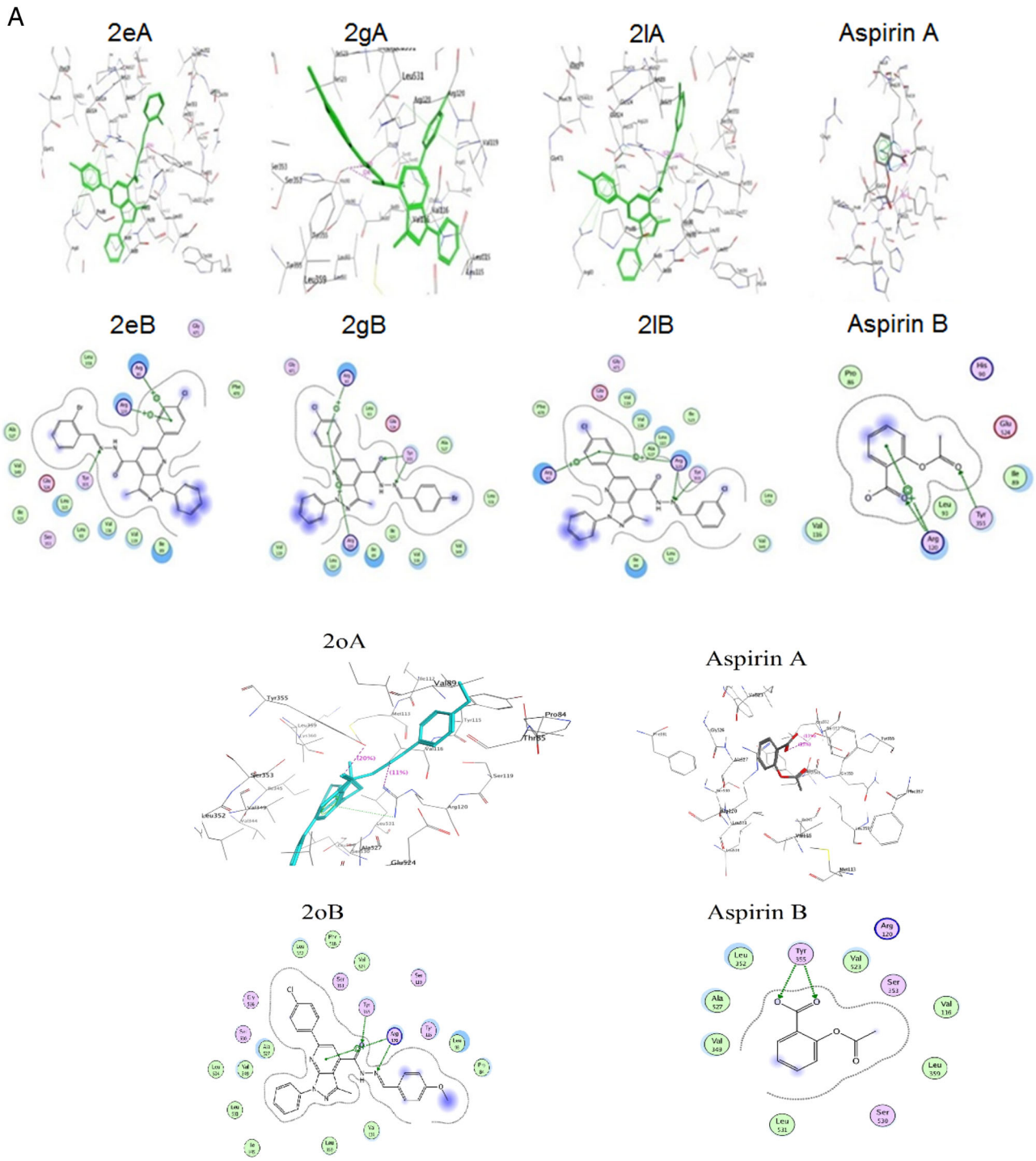

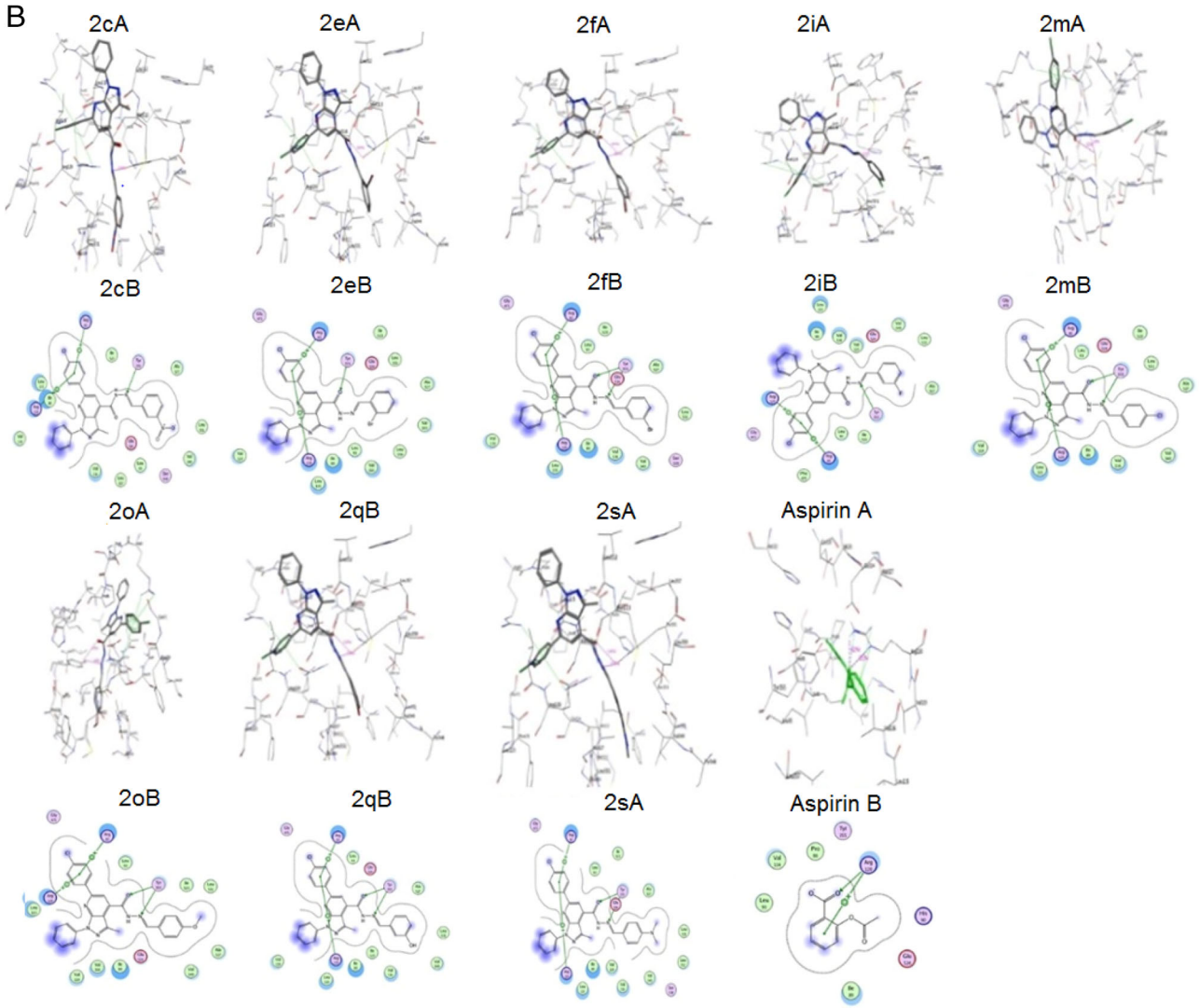

Fig. 2 **a** Two and three dimensional interaction diagrams of **2e**, **2g**, **2l**, **2o** and Aspirin using Naproxen pocket against COX-1 and COX-2. Interaction diagrams were attained by using ligand interaction analysis feature of MOE. **b** Two and three dimensional interaction diagrams of **2c**, **2e**, **2f**, **2i**, **2m**, **2o**, **2q**, **2s** and Aspirin using selected residues. Interaction diagrams were attained by using ligand interaction analysis feature of MOE while Arg120, Arg83, and Tyr355 residue of COX-1 were used

on the nitro-benzylidene unit revealing ICT from 1-phenyl-1*H*-pyrazolo[3,4-*b*]pyridine to nitro-benzylidene moiety. In **2n–2s**, the LUMO is localized on the pyrazolo[3,4-*b*]pyridine. The ICT has been observed from phenyl to the pyrazolo[3,4-*b*]pyridine and chlorophenyl. As in **2b–2d**, the strong electron deactivating group is at ortho, meta, and para positions, respectively as a result nitro-benzylidene moiety withdraw electron toward itself while in **2n–2o**, electron activating group methoxy is substituted in corollary methoxybenzylidene is usually not taking part in the formation of the LUMO. It is expected that strong electron activating group $-N(CH_3)_2$ in 2s is playing significant role by which HOMO is distributed at (dimethyl amino-benzylidene)-hydrazide unit. In Aspirin, the HOMO is distributed at phenol moiety and the LUMO at phenol as well as carboxylic group leading the ICT from phenol to the anchoring site (carboxylic group). In trolox, the HOMO is distributed at conjugated ring along with some charge at –OH and $-CH_3$ groups while the LUMO is localized at whole of the molecule revealing ICT from left to the right side of the system.

In Supporting Supplementary Table S_5, we have tabulated the HOMO energies (E_{HOMO}), LUMO energies (E_{LUMO}), HOMO–LUMO energy gaps (E_{gap}), IP, and EA at the B3LYP/6-31G** level of theory. The E_{HOMO} levels of indigenously synthesized and studied hydrazone derivatives are lower than the trolox while higher than Aspirin while E_{gap} is smaller than the trolox and Aspirin. The largest E_{gap} has been observed for the **2j, 2n–2o** amongst all the hydrazone derivatives. Moreover, with respect to charge

Table 2 (A) Docking result using the selected naproxen pocket for COX-1 and 2 and (B) selected residues

(A)

Compound	Van der Waal forces (kcal/mol)	Interacting residues	Enzyme selected
2e (R = 2Br)	−3.08	Arg83, Arg120, Tyr355	COX-1
2g (R = 4Br)	−21.57	Arg83, Arg120, Tyr355	COX-1
2l (R = 3Cl)	−17.78	Arg83, Arg120, Tyr355	COX-1
Aspirin	−15.61	Arg120, Tyr355	COX-1
2o (R = $2OCH_3$)	−10.72	Arg120, Tyr355	COX-2
Aspirin	−11.48	Tyr355	COX-2

(B)

sp Compound	Van der Waal forces (kcal/mol)	Interacting residues	Enzyme selected
2c (R = $3NO_2$)	−6.58	Arg83, Arg120, Tyr355	COX-1
2e (R = 2Br)	−3.20	Arg83, Arg120, Tyr355	COX-1
2f (R = 3Br)	−14.54	Arg83, Arg120, Tyr355	COX-1
2i (R = 3 F)	−16.48	Arg83, Arg120, Tyr355	COX-1
2m (R = 4Cl)	−17.53	Arg83, Arg120, Tyr355	COX-1
2o (R = $2OCH_3$)	−19.35	Arg83, Arg120, Tyr355	COX-1
2q (R = 3OH)	−12.99	Arg83, Arg120, Tyr355	COX-1

PDB Code = 1Q4G and 3NT1 for COX-1 and COX-2, respectively from already published articles

transfer ability of the compounds, it is expected that the higher EA of **2b–2m** might lead to enhanced electron transport aptitude in these contenders than the **2a**. The scavenging of free radical can be evaluated by single electron donation. IP is an important descriptor by which the range of electron transfer can be assessed. By removing electron from HOMO one-electron transfer radical cation can be gained. It can be seen that **2b**, **2e**, **2h**, **2k**, **2n**, **2o**, and **2t** have the smaller IP values as compared to the parent compound **2a** revealing that in these materials electron transfer mechanism might be more encouraging for the scavenging of free radicals (Supporting Supplementary-Table S5).

Molecular electrostatic potential (MEP)

The 3-D surface maps of the MEP are best tools to know the molecular interactions as well as the relative reactivity sites for the nucleophilic and electrophilic attack. In Fig. 4, we have illustrated the MEP surface maps of hydrazone derivatives from **2a–2t** along with reference compounds to understand the positive and negative electrostatic potential (ESP) regions. In Fig. 4, red, blue and green colors represent the negative, positive and zero potential regions. It is anticipated that the electrophilic and nucleophilic attack would be favorable on the negative and positive ESP. The negative ESP can be seen on the oxygen of C=O and nitrogen of pyrazole in **2a** whereas the positive ESP at benzylidene-hydrazine moiety. Almost analogous tendency has been observed in all the studied derivatives. In **2b–2d**, the negative ESP can also be seen on the nitro group. From this MEP surface maps, it is expected that the oxygen of C=O and nitrogen of pyrazole would be favorable electrophilic reactive sites and benzylidene-hydrazine moiety as a nucleophilic reactive site. Furthermore, in **2b–2d**, the nitro group would be favorable electrophilic reactive site.

QSAR study

Different QSAR descriptors, e.g., μD = dipole moment, area, volume, partition coefficient (Log *P*), hydrogen bond donor (HBD), hydrogen bond acceptor, polar surface area (PSA), solvation energy, and polarizability of hydrazone derivatives have been tabulated in Table 3. Previously, it has been shown that PSA should not exceed 120 A^2 for the orally active drug which are transported by trans cellular route (Kelder 1999; van de Waterbeemd et al. 1998) and <100 A^2 for brain penetration (van de Waterbeemd et al. 1998) or <60–70 A^2 (Kelder et al. 1999). The PSA of all the studied hydrazone derivatives is less than 120 A^2. Moreover, the PSA of all the studied hydrazone (except **2b–2d**) derivatives is also smaller than 60 A^2. On other, lipophilicity of the studied compounds ranges from 5.56 to 8.26. The lipophilicity increases by substituting the electron deactivating groups (–F, –Cl, –Br, and NO_2) while the electron activating group ($–OCH_3$) and furan moiety decreases lipophilicity than parent compound **2a**. From the previous studies, it is widely accepted that the compounds having very high/low log *P* values do not have good bioavailability as they cannot cross hydrophilic and lipophilic barricades, respectively. However, these compounds might be used as lead compounds to synthesize better antiplatelet

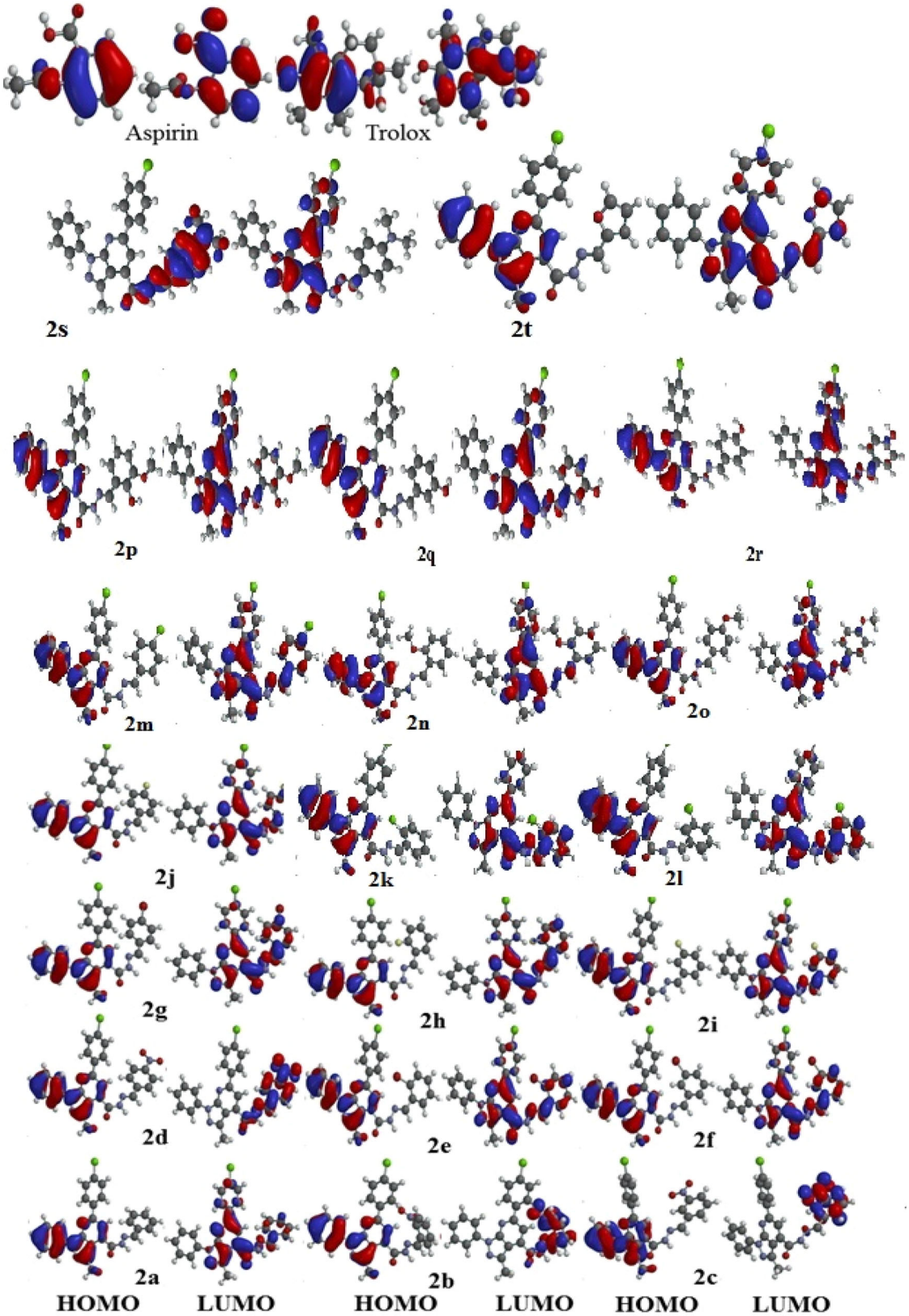

Fig. 3 The distribution pattern of the HOMOs and LUMOs of the studied compounds (**2a–2t**) at ground states

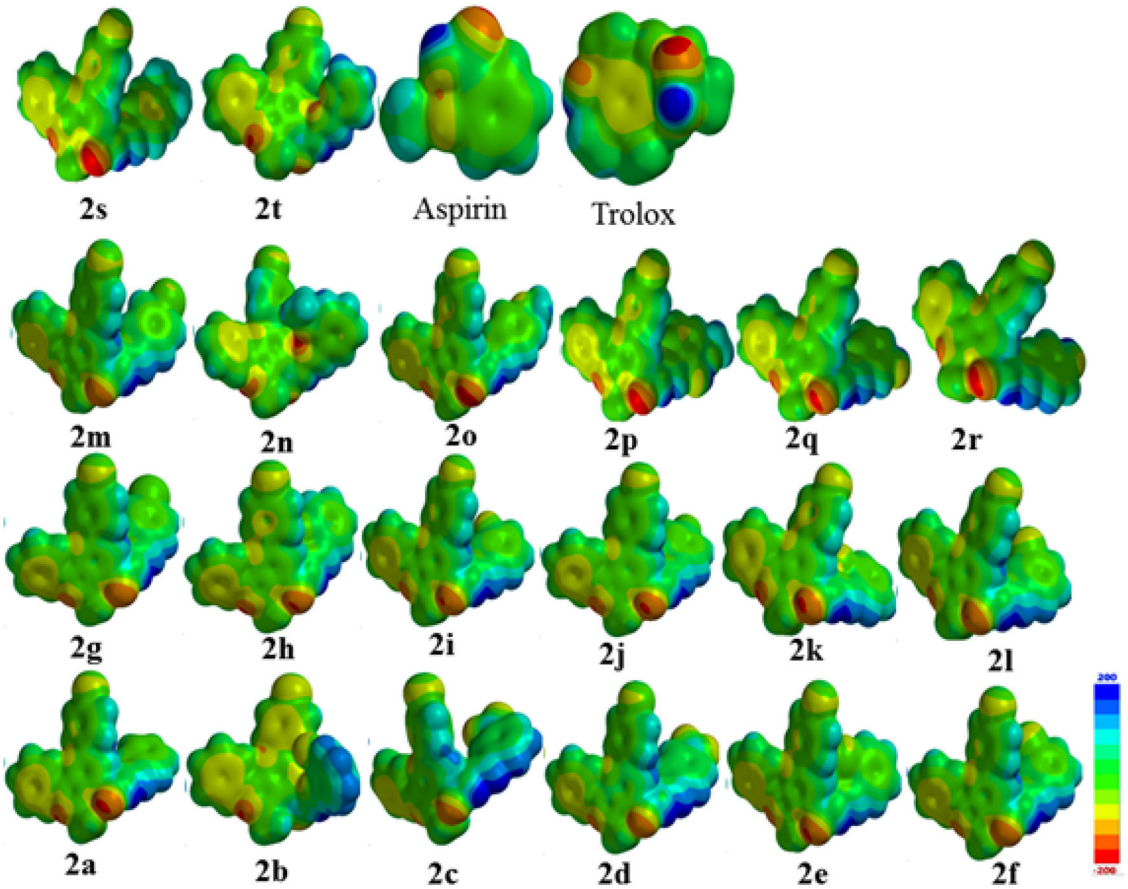

Fig. 4 The molecular electrostatic potential surfaces of the *N′*-benzylidene derivatives (**2a–2t**). Red, blue and green color regions represented the negative, positive and zero electrostatic potential of derivative (**2a–2t**) (color figure online)

Table 3 Different QSAR descriptors of (**2a–2t**) obtained at B3LYP/6-31 G** level of theory

	μD (Debye)	Area (A^2)	Volume (A^3)	Log P	HBD	HBA	Pol.	PSA (A^2)	S.E. (KJ/mol)
2a	4.92	479.29	462.52	7.43	0	6	78.02	47.51	−28.37
2b	8.77	502.94	484.27	7.46	1	9	79.97	85.16	−45.2
2c	6.94	505.38	484.15	7.46	1	9	79.9	86.70	−43.31
2d	4.18	505.22	484.11	7.46	1	9	79.54	86.61	−34.97
2e	6.02	491.56	480.19	8.26	1	6	79.47	46.49	−32.11
2f	5.41	499.8	480.69	8.26	1	6	79.51	47.69	−33.27
2g	3.81	499.7	480.66	8.26	1	6	79.5	47.62	−31.09
2h	6.18	482.9	466.87	7.59	1	6	78.39	46.05	−31.46
2i	5.23	485.15	467.14	7.59	1	6	78.41	47.60	−27.05
2j	4.18	485.12	467.14	7.59	0	6	78.39	47.59	−24.95
2k	6.24	493.46	476.10	7.99	1	6	79.14	46.96	−32.62
2l	5.40	495.22	476.25	7.99	1	6	79.15	47.65	−31.8
2m	3.82	495.2	476.24	7.99	1	6	79.14	47.65	−29.57
2n	5.24	506.42	489.39	7.30	0	7	80.20	52.60	−32.44
2o	6.99	509.10	489.62	7.14	0	7	80.21	54.50	−35.38
2p	7.91	515.79	496.44	6.75	1	8	80.76	70.95	−38.73
2q	5.31	488.19	469.62	7.04	1	7	78.59	67.22	−48.77
2r	4.61	488.15	469.60	7.04	1	7	78.59	67.21	−49.24
2s	8.08	530.67	511.76	7.67	0	7	82.09	48.34	−33.65
2t	5.83	460.01	440.96	5.56	1	7	76.29	54.91	−32.89
Aspirin	2.65	196.35	174.86	1.18	1	7	54.25	51.99	−33.03
Trolox	2.78	275.19	264.27	4.29	2	2	61.50	49.81	−34.81

μD dipole moment, *HBD* hydrogen bond donor, *HBA* hydrogen bond acceptor, *PSA* polar surface area, *S.E.* solvation energy, *Pol.* polarizability

agents with good log *P* value. Similar compounds have been reported in literature having better biological activities with high log *P* value (Dias et al. 2007).

Conclusion

In summary, we evaluated the potential of novel *N*′-benzylidene-3-methyl-1-phenyl-6-*p*-chlorophenyl-1*H*-pyrazolo [3,4*b*]pyridine-4carbohydrazides **(2a–2t)** as new antithrombotic agents. These compounds were synthesized starting from the simple chemicals via functional group replacement approach and their structures were elucidated by various spectroscopic techniques. All compounds except of **2c**, **2f, 2t** have exhibited high antioxidant potential and compounds (**2c**, **2e**, **2f**, **2g**, **2i**, **2m**, **2o, 2q**) have showed superlative antiplatelet activity, respectively. Docking results revealed that compounds involved in the hydrogen bond formation with the interacting residues for antiplatelet activity against (COX-1 and COX-2) and were found in accordance with the experimental results. QSAR results are in good agreement with antiplatelet and antioxidant activities of the compounds (**2a–2t**). Our finding suggest that the **2g**, **2l** and **2m** might be promising antiplatelet agents and will be helpful in the designing of new drugs for the treatment of cardiovascular, thromboembolic, and anti-inflammatory diseases.

Acknowledgements We are thankful to Higher Education Commission of Pakistan for research funding Indigenous 5000 PhD fellowship Batch VII (PIN # 117-6703-PS7-083) and Ex-Supervisor Professor Dr. Riffat Parveen (Late) for her countless efforts. Professor Dr. Makshoof Athar, Director, Institute of Chemistry, University of the Punjab, Lahore for his support and providing facilities to carry on this research work. We are also thankful to University of Health Sciences, Lahore for providing the Elisa reader and platelet counter facility.

Compliance with ethical standards

Conflict of interest The authors declare that they have no competing interests.

References

Abdel-Wahab BF, Awad GE, Badria FA (2011) Synthesis, antimicrobial, antioxidant, anti-hemolytic and cytotoxic evaluation of new imidazole-based heterocycles. Eur J Med Chem 46 (5):1505–1511

Abdelazem AZ, Al-Sanea MM, Park BS, Park HM, Yoo KH, Sim T, Lee SH (2015) Synthesis and biological evaluation of new pyrazol-4-ylpyrimidine derivatives as potential ROS1 kinase inhibitors. Eur J Med Chem 90:195–208

Abu-Surrah AS, Safieh KAA, Ahmad IM, Abdalla MY, Ayoub MT, Qaroush AK, Abu-Mahtheieh AM (2010) New palladium (II) complexes bearing pyrazole-based Schiff base ligands: Synthesis, characterization and cytotoxicity. Eur J Med Chem 45 (2):471–475

Ahad A, Ahmad A, ud Din S, Rao AQ, Shahid AA, Husnain T (2015). In silico study for diversing the molecular pathway of pigment formation: an alternative to manual coloring in cotton fibers. Front Plant Sci 6:751. http://doi:10.3389/fpls.2015.00751

Ahmad A, Ahad A, Rao AQ, Husnain T (2015) Molecular docking based screening of neem-derived compounds with the NS1 protein of Influenza virus. Bioinformation 11(7):359–65

Ahmad A, Javed MR, Rao AQ, Khan MA, Ahad A, ud Din S et al. (2015) In-silico determination of insecticidal potential of Vip3Aa-Cry1Ac fusion protein against lepidopteran targets using molecular docking. Front Plant Sci 6:1081. http://doi:10.3389/fpls.2015.01081

Ajani OO, Obafemi CA, Nwinyi OC, Akinpelu DA (2010) Microwave assisted synthesis and antimicrobial activity of 2-quinoxalinone-3-hydrazone derivatives. Bioorg Med Chem 18(1):214–221

Al-Sehemi AG, Irfan A, Alfaifi M, Fouda AM, Ma'mon El-Gogary T & Ibrahim DA (2017) Computational study and in vitro evaluation of the anti-proliferative activity of novel naproxen derivatives. J King Saud Univ Sci. https://doi.org/10.1016/j.jksus.2017.01.003

Al-Sehemi AG, Irfan A, Aljubiri SM, Shaker KH (2012) Density functional theory investigations of radical scavenging activity of 3′-Methyl-quercetin. J Saudi Chem Soc. https://doi.org/10.1016/j.jscs.2012.08.004

Al-Sehemi AG, Irfan A, Alrumman SA, HeshamA AE-L (2016) Antibacterial activities, dft and qsar studies of quinazolinone compounds. Bull Chem Soc Ethiop 30(2):307–316

Baylac S, Racine P (2003) Inhibition of 5-lipoxygenase by essential oils and other natural fragrant extracts. Int J Aromather 13 (2):138–142

Belcastro M, Marino T, Russo N, Toscano M (2006) Structural and electronic characterization of antioxidants from marine organisms. Theor Chem Acc 115(5):361–369. https://doi.org/10.1007/s00214-006-0077-5

Bezerra-Netto HJ, Lacerda DI, Miranda ALP, Alves HM, Barreiro EJ, Fraga CA (2006) Design and synthesis of 3, 4-methylenedioxy-6-nitrophenoxyacetylhydrazone derivatives obtained from natural safrole: new lead-agents with analgesic and antipyretic properties. Bioorg Med Chem 14(23):7924–7935

Bock K, Pedersen C (1974) A study of 13 CH coupling constants in hexopyranoses. J Chem Soc Perkin Trans 2(3):293–297

Chaudhry AR, Ahmed R, Irfan A, Muhammad S, Shaari A, Al-Sehemi AG (2014) Effect of heteroatoms substitution on electronic, photophysical and charge transfer properties of naphtha [2,1-b:6,5-b′] difuran analogues by density functional theory. Comput Theor Chem 1045(0):123–134. https://doi.org/10.1016/j.comptc.2014.06.028

Chaudhry AR, Ahmed R, Irfan A, Shaari A, Maarof H, Al-Sehemi AG (2014) First principles investigations of electronic, photoluminescence and charge transfer properties of the Naphtho [2, 1-b: 6, 5-b′] difuran and its derivatives for OFET. Sains Malays 43 (6):867–875

de Aguiar Cordeiro R, de Melo CVS, de Farias Marques FJ, Serpa R, de Jesus Evangelista AJ, Caetano EP, Bandeira TdJPG (2016) Synthesis and in vitro antifungal activity of isoniazid-derived hydrazones against Coccidioides posadasii. Microb Pathog 98:1–5

Dias LR, Santos MB, de Albuquerque S, Castro HC, de Souza AM, Freitas AC, Rodrigues CR (2007) Synthesis, in vitro evaluation, and SAR studies of a potential antichagasic 1H-pyrazolo [3, 4-b] pyridine series. Bioorg Med Chem 15(1):211–219

Fraser RR, Banville J, Akiyama F, Chuaqui-Offermanns N (1981) 13C shieldings in syn and anti aldimines and ketimines. Can J Chem 59(4):705–709

Frisch MJ, Trucks GW, Schlegel HB et al. (2009) Gaussian-09, Revision A.1. Gaussian, Inc., Wallingford, CT

Geraldo R, Bello M, Dias L, Vera M, Nagashima T, Abreu P, Freitas A (2010) Antiplatelet activity and structure-activity relationship study of Pyrazolopyridine Derivatives as potential series for treating thrombotic diseases. J Atheroscler Thromb 17(7): 730–739

Glidewell C, Low JN, Skakle JM, Wardell JL (2004a) Hydrogen-bonded dimers in 2-nitrobenzaldehyde hydrazone and a three-dimensional hydrogen-bonded framework in 3-nitrobenzaldehyde hydrazone. Acta Crystallogr C60(9):o686–o689

Glidewell C, Low JN, Skakle JM, Wardell JL (2004b) Hydrogen bonding in nitroaniline analogues: 4-nitrobenzaldehyde hydrazone forms hydrogen-bonded sheets of R_ {\ bf 4}^{\ bf 4}(26) rings. Acta Crystallogr C 60(1):o33–o34

Haj Mohammad Ebrahim Tehrani K, Sardari S, Mashayekhi V, Esfahani Zadeh M, Azerang P, Kobarfard F (2013) One pot synthesis and biological activity evaluation of novel Schiff bases derived from 2-hydrazinyl-1, 3, 4-thiadiazole. Chem Pharm Bull 61(2):160–166

Himmelreich U, Häßner R, Thomas P, Tschwatschal F, Borsdorf R (1990) NMR-spektroskopische Untersuchungen zurE/Z-Isomerie von substituierten Dithiocarbazinsäurederivaten. Monatsh Chem 121(11):923–930

Himmelreich U, Tschwatschal F, Borsdorf R (1993) NMR-spektroskopische untersuchungen an derivaten des 2, 4-Dichlorphenoxyessigsäurehydrazids. Monatsh Chem 124 (10):1041–1051

Hutter M (2009) In silico prediction of drug properties. Curr Med Chem 16(2):189–202

Irfan A, Al-Sehemi AG (2014) DFT study of the electronic and charge transfer properties of perfluoroarene–thiophene oligomers. J Saudi Chem Soc 18(5):574–580. https://doi.org/10.1016/j.jscs.2011.11.006

Irfan A, Al-Sehemi AG, Chaudhry AR, Muhammad S, Asiri AM (2016) The structural, electro-optical, charge transport and nonlinear optical properties of 2-[(3,5-dimethyl-1-phenyl-1H-pyrazol-4-yl)methylidene]indan-1,3-dione. Optik 127(21): 10148–10157. https://doi.org/10.1016/j.ijleo.2016.08.007

Irfan A, Kalam A, Chaudhry AR, Al-Sehemi AG, Muhammad S (2017) Electro-optical, nonlinear and charge transfer properties of naphthalene based compounds: a dual approach study. Optik 132:101–110. https://doi.org/10.1016/j.ijleo.2016.12.023

Karmakar A, Singh B (2017) Spectroscopic and theoretical studies of charge-transfer interaction of 1-(2-pyridylazo)-2-napthol with nitroaromatics. Spectrochim Acta A Mol Biomol Spectrosc 179:110–119

Kelder J, Grootenhuis PJ, Bayada D, Delbressine LC, Ploemen J-P (1999) Polar molecular surface as a dominating determinant for oral absorption and brain penetration of drugs. Pharm Res 16 (10):1514–1519. https://doi.org/10.1023/a:1015040217741

Koop B, Straub A, Schäfer HJ (2001) Stereoselective oxidation of 4-aryl-1, 4-dihydropyridines to axially chiral 4-arylpyridines with 2, 2, 6, 6-tetramethyl-1-oxopiperidinium tetrafluoroborate (TEMPO +BF 4−). Tetrahedron Asymmetry 12(2):341–345

Li J, Li J, Jiao Y, Dong C (2014) Spectroscopic analysis and molecular modeling on the interaction of jatrorrhizine with human serum albumin (HSA). Spectrochim Acta A Mol Biomol Spectrosc 118:48–54

Magda A-A, Abdel-Aziz NI, Alaa A-M, El-Azab AS, Asiri YA, ElTahir KE (2011) Design, synthesis, and biological evaluation of substituted hydrazone and pyrazole derivatives as selective COX-2 inhibitors: Molecular docking study. Bioorg Med Chem 19(11):3416–3424

Nakka M, Begum M, Varaprasad B, Reddy L, Bhattacharya A, Helliwell M, Mukkanti K (2010) Naproxen and ibuprofen based acyl hydrazone derivatives: Synthesis, structure analysis and cytotoxicity studies. J Chem Pharm Res 2(393409):29

Narsinghani T, Sharma MC, Bhargav S (2013) Synthesis, docking studies and antioxidant activity of some chalcone and aurone derivatives. Med Chem Res 22(9):4059–4068

Palla G, Pelizzi C, Predieri G & Vignali C (1982) Conformational study on N-acylhydrazones of aromatic-aldehydes by nmr-spectroscopy. Gazz chim Ital 112:339–341

Palla G, Predieri G, Domiano P, Vignali C, Turner W (1986) Conformational behaviour and E/Z isomerization of N-acyl and N-aroylhydrazones. Tetrahedron 42(13):3649–3654

Patole J, Sandbhor U, Padhye S, Deobagkar DN, Anson CE, Powell A (2003) Structural chemistry and in vitro antitubercular activity of acetylpyridine benzoyl hydrazone and its copper complex against Mycobacterium smegmatis. Bioorg Med Chem Lett 13(1):51–55

Patorski P, Wyrzykiewicz E. & Bartkowiak G. (2012) Synthesis and conformational assignment of N-(E)-stilbenyloxymethylenecarbonyl-substituted hydrazones of acetone and o-(m- and p-) chloro-(nitro-) benzaldehydes by means of and NMR spectroscopy. J Spectrosc2013

Reddy MVB, Shen Y-C, Yang J-S, Hwang T-L, Bastow KF, Qian K, Wu T-S (2011) New bichalcone analogs as NF-κB inhibitors and as cytotoxic agents inducing Fas/CD95-dependent apoptosis. Bioorg Med Chem 19(6):1895–1906

Salgın-Gökşen U, Gökhan-Kelekçi N, Göktaş Ö, Köysal Y, Kılıç E, Işık Ş, Özalp M (2007) 1-Acylthiosemicarbazides, 1, 2, 4-triazole-5 (4H)-thiones, 1, 3, 4-thiadiazoles and hydrazones containing 5-methyl-2-benzoxazolinones: synthesis, analgesic-anti-inflammatory and antimicrobial activities. Bioorg Med Chem 15(17):5738–5751

Seleem HS, El-Inany GA, El-Shetary BA, Mousa MA (2011) The ligational behavior of a phenolic quinolyl hydrazone towards copper (II)-ions. Chem Cent J 5(1):2

Singh M, Raghav N (2011) Biological activities of hydrazones: a review. Int J Pharm Pharm Sci 3(4):26–32

Srikala P, Tarafder K, Trivedi DR (2017) Design and synthesis of a new organic receptor and evaluation of colorimetric anion sensing ability in organo-aqueous medium. Spectrochim Acta A Mol Biomol Spectrosc 170:29–38

Sriram D, Yogeeswari P, Madhu K (2005) Synthesis and in vitro and in vivo antimycobacterial activity of isonicotinoyl hydrazones. Bioorg Med Chem Lett 15(20):4502–4505

Storey R, Wilcox R, Heptinstall S (1998) Differential effects of glycoprotein IIb/IIIa antagonists on platelet microaggregate and macroaggregate formation and effect of anticoagulant on antagonist potency implications for assay methodology and comparison of different antagonists. Circulation 98(16):1616–1621

Syakaev VV, Podyachev SN, Buzykin BI, Latypov SK, Habicher WD, Konovalov AI (2006) NMR study of conformation and isomerization of aryl-and heteroarylaldehyde 4-tert-butylphenoxyacetylhydrazones. J Mol Struct 788(1):55–62

van de Waterbeemd H, Camenisch G, Folkers G, Chretien JR, Raevsky OA (1998) Estimation of blood-brain barrier crossing of drugs using molecular size and shape, and H-bonding descriptors. J Drug Target 6(2):151–165. https://doi.org/10.3109/10611869808997889

Wright JS, Johnson ER, DiLabio GA (2001) Predicting the activity of phenolic antioxidants: theoretical method, analysis of substituent effects, and application to major families of antioxidants. J Am Chem Soc 123(6):1173–1183. https://doi.org/10.1021/ja002455u

Wyrzykiewicz E, Błaszczyk A, Turowska-Tyrk I (2000) N-(E)-2-stilbenyloxymethylenecarbonyl substituted hydrazones of ortho, meta and para hydroxybenzaldehydes. Bull Pol Acad Sci Chem 48(3):213–229

Wyrzykiewicz E, Prukala D (1998) New isomeric N-substituted hydrazones of ortho, meta and para hydroxybenzaldehydes. Pol J Chem 72(4):694–702